RESEARCH ARTICLE

VOLCANICA

Calcite-saturated natrocarbonatites: composition, crystal morphology, and weathering

Michael Anenburg*[α] and Izzan Nur Aslam[β]

[α] Research School of Earth Sciences, Australian National University, Canberra ACT 2600, Australia.
[β] Department of Mining Engineering, Universitas Syiah Kuala, Aceh 23111, Indonesia.

Abstract

Interpretation of calcite-dominated fossil carbonatite volcanoes is complicated by the instability of many igneous carbonatite minerals on Earth's surface. One hypothesis suggests that they originate by eruption of alkali-free calcic carbonatite lavas. However, liquid calcite is not thermodynamically stable at atmospheric pressure. A second hypothesis suggests that calcite is secondary and formed after magmatic alkali carbonate minerals, primarily nyerereite, lost their Na or K to surface water. Here, we experimentally test a combined hypothesis in which solid calcite phenocrysts are suspended in natrocarbonatite lava that solidifies primarily to nyerereite, and determine calcite solubilities in sodic carbonate liquids. Then, we dissolve alkalis in water over several months to show formation of secondary calcite after nyerereite. Textural and geochemical observations from our experiments are consistent with many natural volcanic carbonatites. Magmatic calcite occurs as rounded and elongated subhexagonal prisms, whereas secondary calcite exhibits a range of fine-grained morphologies. Magmatic calcite only contains Sr as a significant minor element, whereas secondary calcite is chemically diverse with Na, K, P, and Ba as important minor elements. Strontium is also present in secondary calcite, but in lower concentrations than primary magmatic calcite. Calcite types with both primary and secondary characteristics occur in many natural carbonatites, indicating that alteration of initially calcite–nyerereite-bearing natrocarbonatites to calcite carbonatites was more common in Earth's geological past than previously recognised.

Keywords: Carbon cycle; Calciocarbonatite; Experimental petrology; Sövite; Weathered carbonatite; Pyroclastic flow.

Submitted: 2024-02-20 | Accepted: 2024-09-17 | Published: 2024-11-25

Editor: Sami Mikhail | Typesetter: Gareth N. Fabbro

1 Introduction

It is well known that carbonatite rocks do not represent the carbonatite melt compositions from which they formed [Le Bas 1981; Mitchell 2005; Guzmics et al. 2011; Kamenetsky et al. 2021; Yaxley et al. 2022]. That these are essentially cumulate rocks has been repeatedly demonstrated for the common intrusive calcite and dolomite carbonatites [Veksler et al. 1998; Anenburg et al. 2020; Chayka et al. 2021], with cumulate processes governed mostly by non-gravitational processes. In contrast, there has been some expectation for the less abundant extrusive carbonatites to preserve most of their primary character, similar to how silicate lava flows and tuffs faithfully record their liquid compositions [Katz and Keller 1981; Keller 1989; Bailey 1990; Mourão et al. 2010; Toscani et al. 2020], although synmagmatic alkali loss has been suggested [Macdonald et al. 1993; Eby et al. 2009]. However, solidified carbonatite lavas are infamous for their instability, as shown by the natrocarbonatites[†] of the Oldoinyo Lengai volcano in Tanzania, the only currently known active carbonatite volcano [Dawson 1962]. Within minutes, these lavas begin to react with atmospheric moisture, and they experience rapid dissolution in meteoric water [Hay 1989; Keller and Krafft 1990; Zaitsev and Keller 2006]. The residual material substantially differs from the primary carbonatite melt crystallisation products in terms of its geochemistry, mineral assemblage, and potentially microstructures.

1.1 Origins of extrusive calcite carbonatites

How does one, given the potential ephemerality of alkali-bearing carbonatite lavas, interpret a geologically historical extrusive carbonatite [Barker 1989; Keller and Zaitsev 2006]? The overwhelming majority of extrusive carbonatites are dominated by calcite, which led some researchers to speculate that these were originally calcic melts [von Knorring and du Bois 1961; Dawson 1964b; Keller 1981; Hayward and Jones 1991; Stoppa and Cundari 1995; Mitchell and Dawson 2021], with calcite grains crystallising as phenocrysts or as the matrix material [Keller 1989]. This hypothesis overlooks the fact that the refractory nature of calcite in anhydrous settings, as expected in dehydrated lavas at the surface, was one of the arguments against the igneous origin of carbonatites in the first half of the 20th century [see discussion in Pecora 1956; Wyllie and Tuttle 1960], and that liquid calcite cannot exist at Earth's surface pressures (although carbonatite melts can exist to pressure as low as 10 bar, equivalent to a few tens of metres depth underground [Wyllie and Tuttle 1962; Wyllie and Raynor 1965]). Alternatively, some suggested that calcite was a deeply sourced antecryst or an in-situ formed phenocryst, suspended within a natrocarbonatite lava, with the sodic lava altering to calcite of a second generation [Hay 1983; Mariano and Roeder 1983; Deans and Roberts 1984; Rosatelli et al. 2010; Zaitsev 2010; Lundstrom et al. 2022]. This hypothesis is dif-

* michael.anenburg@anu.edu.au

[†] We use the term "natrocarbonatite" to refer to Na-rich carbonatite melts which primarily solidify to Na-carbonate minerals, often nyerereite. The Oldoinyo Lengai natrocarbonatites also form gregoryite, reflecting their exceptional Na contents. However, our usage of "natrocarbonatite" does not require chemical similarity to the Oldoinyo Lengai lavas or presence of abundant gregoryite.

ficult to test in nature because Oldoinyo Lengai, the only active carbonatite volcano, has no calcite phenocrysts [Dawson 1989; Guzmics et al. 2019]. Instead, the $CaCO_3$ component of its melt is present as a minor component in gregoryite and nyerereite solid solutions [Keller and Zaitsev 2006; Berkesi et al. 2020; Baudouin and France 2023]. A third option is that all calcite is secondary, forming in low temperature conditions after all or most alkali carbonates have been dissolved, similar to the actual process happening now at Oldoinyo Lengai [Zaitsev and Keller 2006; Campeny et al. 2015].

1.2 Calcite phenocrysts in natrocarbonatite liquids?

Oldoinyo Lengai is only one volcano that does not represent all possible extrusive carbonatite melt compositions, as observed by Le Bas [1981, 1987] who highlighted the difference between the calcite-free Oldoinyo Lengai natrocarbonatite and the other calcite-dominated extrusive carbonatites. Melt inclusion studies of intrusive calcite and dolomite carbonatites unequivocally demonstrate that they crystallise in equilibrium with alkali-rich carbonatite melts [Veksler et al. 1998; Guzmics et al. 2011; Chen et al. 2013; Káldos et al. 2015; Prokopyev et al. 2020; Chayka et al. 2021; Prokopyev et al. 2021], a fact supported by formation of calcite in experiments of alkaline carbonatites [Weidendorfer et al. 2017; Anenburg et al. 2020]. We see no reason why these calcite-saturated yet alkali carbonatite melts cannot erupt at the surface. Additional calcite can crystallise directly from the natrocarbonatite liquid if the temperature is below the calcite decomposition temperature [Gittins and Jago 1991]. Many extrusive carbonatites contain clear tabular calcite, as well as turbid calcite which appears to pseudomorph another mineral (presumably nyerereite or melilite), and a fine-grained calcite groundmass [e.g. Turner 1988; Hayward and Jones 1991; Rosatelli et al. 2003; Andersen 2008; Campeny et al. 2015; Mitchell and Dawson 2021]. If the clear tabular calcite crystals are indeed phenocrysts, then calcite-saturated natrocarbonatites are much more common than the highly alkaline and gregoryite-saturated Oldoinyo Lengai carbonatites. Clearly, the high temperature calcite phenocryst hypothesis is feasible, but distinguishing it from low temperature secondary calcite is difficult, often requiring cathodoluminescence or in-situ isotopic analysis methods to resolve small-scale spatial differences [Stoppa et al. 2023]. There is much debate on the topic based on observations from natural systems [e.g. Turner 1988; Ngwenya and Bailey 1990; Gittins and Harmer 1997; Keller and Zaitsev 2006; Mitchell and Dawson 2021], with inconclusiveness exacerbated by an experimental gap on these systems. This study aims to shed some light on this topic and provide constraints on natrocarbonatite characteristics, such that natural extrusive carbonatites are easier to interpret.

1.3 Experimental approach

Bailey [1993] said that "*Obviously, alkali melts with a calcite liquidus may exist… Actual alkali carbonate melts with calcite phenocrysts have yet to be observed in nature, and their existence still awaits confirmation.*" This hypothesis has remained untested for three decades (notwithstanding preliminary results by Gittins and Jago [1991]). Even recently, Rapprich et al. [2024] noted the apparent conundrum whereby $CaCO_3$ is not stable in hot surface conditions, and suggested that rapid eruption may be required to preserve primary calcite crystals. Pure $CaCO_3$ (i.e. calcite) is indeed unstable at sufficiently hot temperatures: the decomposition temperature in 1 atm CO_2 gas is around 900 °C [Galan et al. 2012], with lower temperatures in natural-like atmospheres or lower pressures (such as on mountain tops). Whilst molten calcite cannot exist on the surface, Ca^{2+} cations or $CaCO_3$ as a thermodynamic component can be dissolved in an alkali mixed-cation carbonate liquid (i.e. a natrocarbonatite). Natrocarbonatite lavas can erupt in temperatures as low as 600 °C, leaving a 300 °C temperature gap in which calcite is a perfectly stable mineral and can potentially carried by or form as a phenocryst from natrocarbonatite lavas. It also seems likely that when these natrocarbonatite lavas are altered, alkalis will be removed with calcite potentially crystallising from the $CaCO_3$-rich residue. Currently, $CaCO_3$ solubilities in natrocarbonatites and their variation with temperature are unknown.

Given that observation of erupting calcite-bearing carbonatite lavas may not occur in our lifetimes, an experimental approach is of value. Here, we conduct high temperature experiments to demonstrate the existence of calcite-saturated natrocarbonatite lavas, and we measure their composition. We also run experiments above the decomposition temperature of calcite [Galan et al. 2012] to examine the possibility of hot lavas which carry initially stable calcite from depth into conditions above its stability limit [cf. Barker 2007]. We also examine the morphology of calcite phenocrysts that form in our experiments and of euhedral calcite rhombs to test whether they retain their shape in igneous systems. Finally, we examine the products of lava dissolution, and whether calcite morphology and composition differ between high temperature calcite and calcite formed as secondary replacement.

2 Methods

2.1 High-temperature experiments

In order to create a natural-like natrocarbonatite lava composition saturated with calcite, we first prepared a chemical mix loosely inspired by published Oldoinyo Lengai compositions [e.g. Dawson 1962; Du Bois et al. 1963; Dawson 1989; Dawson et al. 1990; Keller and Krafft 1990]. Chemical compounds were mixed in an agate mortar and pestle while immersed in acetone until homogeneity (Table 1). The Ca-free natrocarbonatite mix was then mixed with powdered $CaCO_3$ at a natrocarbonatite:$CaCO_3$ ratio of 30:70. This ratio was selected to ensure calcite saturation and constrain $CaCO_3$ solubility in the melt. The combined mix was packed into alumina crucibles and placed in a 120 °C oven to remove all moisture and acetone residue. Two experiments contained additional mm-sized cleavage fragments of calcite obtained from calcite pegmatite veins found along the road in the Cloncurry district, Queensland, Australia. High temperature experiments were conducted in a vertical 1 atm gas mixing furnace. The alumina crucibles were placed inside a platinum bucket attached to an alumina rod (Figure 1). The alumina rod was lowered through an opening at the top of the furnace into the hotspot,

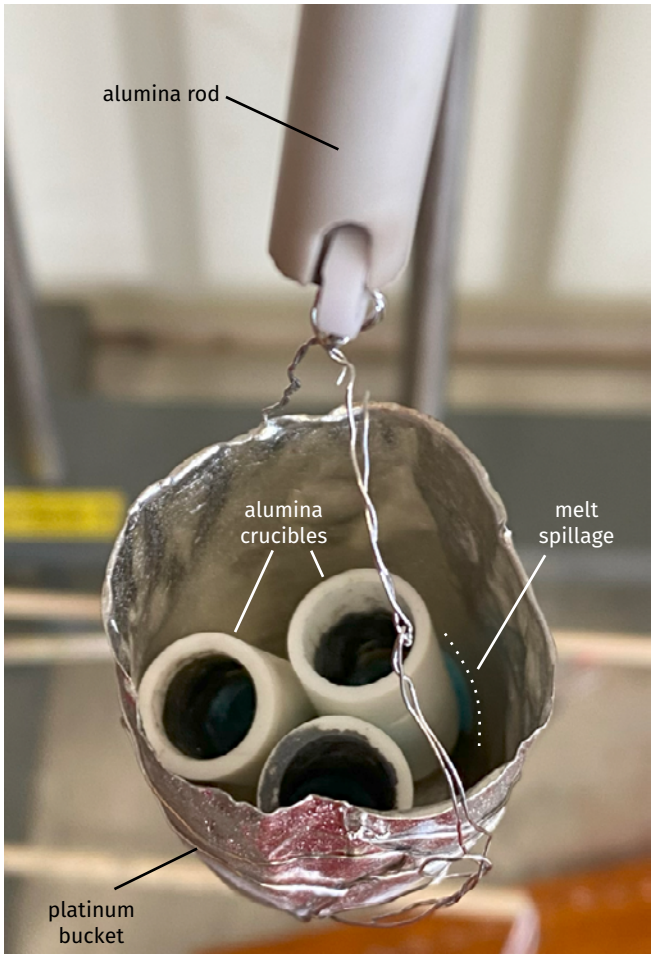

Figure 1: Experimental setup after an experiment, showing three alumina crucibles inside a platinum bucket, hanging from an alumina ring using platinum wire, and suspended below an alumina rod. Minor melt loss is observed as the teal material at the bottom of the bucket.

idling at 600 °C. Preliminary experiments revealed that the sudden temperature increase to 600 °C resulted in some minor melting and exceptionally rapid expansion of gas bubbles trapped in the incipient melt. Together with the excellent wetting characteristics of the melt on the alumina crucibles, this caused catastrophic spraying and loss of material. We resolved this issue by slow and controlled heating of the loaded alumina crucibles in a box furnace. The crucibles were taken out of the box furnace at 500 °C and demonstrated substantial sintering and volume loss. We crushed and repacked the starting mix, then repeated the process at 600 °C after which the crucibles were loaded into the 1 atm gas mixing furnace. Once inside, temperature was increased to the target temperature at 3 °C min^{-1} and dwelled for two hours. The atmosphere inside the furnace was pure CO_2, supplied at a rate of 100 cm^3 min^{-1}. Oxygen fugacity was not strictly buffered, but we estimate conditions to be between the nickel–nickel oxide (NNO) and magnetite–hematite (MH) buffers. After each experiment was complete, the alumina rod was pulled up from the top of the furnace and the bottom of the platinum bucket was briefly dipped in water to expedite the cooling rate. The

Table 1: Synthetic Ca-free natrocarbonatite composition, showing chemical compounds and resulting bulk composition in terms of chemical components.

Compound	Percentage	Component	Percentage
$MnSO_4$	4.07	MnO	1.91
MgF_2	5.12	MgO	3.80
$BaSO_4$	2.60	BaO	1.71
Na_2CO_3	55.83	Na_2O	35.43
K_2CO_3	20.31	K_2O	14.62
NaCl	5.25	SrO	2.28
$Mg_3(PO_4)_2$	1.35	SO_3	5.46
$SrSO_4$	4.04	P_2O_5	0.86
K_2SO_4	1.43	F	3.12
		Cl	3.18
		CO_2	29.65
		–O = (F, Cl)	−2.03
Total	100.00	Total	100.00

In addition to these major components, we also added about 400 ppm of La and 300 ppm of Y.

alumina crucibles were cold enough to the touch within several minutes. Despite pre-heating the crucibles, minor melt spillage and loss was observed in some experiments, where solidified melt was deposited at the bottom of the platinum bucket (Figure 1).

After each experiment, the alumina crucible was mounted in epoxy resin, and once cured, sliced into two halves using a water-cooled saw in about two seconds. Any water was immediately wiped and the samples were placed in a 120 °C oven to dry, after which the sections were again mounted in epoxy resin. Within a day of curing, the first set of sections (Figure 2A–2D) was polished with sandpaper followed by diamond polishing in steps down to 0.25 µm, carbon coated, and taken to electron microscopy for textural and chemical analysis.

We used a Hitachi 4300 SE/N Schottky field emission scanning electron microscope (FE-SEM) equipped with an Oxford Instruments INCA X-MAX energy dispersive spectroscopy (EDS) system employing an 80 mm^2 silicon drift detector (SDD). Images were taken in both secondary electron (SE) and backscattered electron (BSE) modes. The EDS system is calibrated with reference materials, allowing estimation of CO_2 contents of the various phases. Analysis was conducted with 15 kV accelerating voltage and 0.6 nA beam current. Typically, a focused beam was rastered over an area of several tens of µm^2 to minimise alkali loss [Anenburg et al. 2020; Anenburg and Guzmics 2023].

Element mapping was conducted using a JEOL 8530F Plus electron probe microanalyser (EPMA). We used four wavelength dispersive spectrometers (WDS) with operating conditions of 15 kV accelerating voltage, 50 nA beam current, 1 µm beam diameter. Mapping was conducted at a step size of 2.4 µm and 50 ms dwell time. The four elements analysed were Na and Mg using their Kα lines on a TAP crystal, Ca using its Kα line on a PET crystal, and Sr using its Lα line on a PET crystal.

Table 2: List of experiments reported in this study.

Experiment	Temperature (°C)	Added calcite?
1	750	no
2	800	no
3	850	no
4	850	yes
5	950	no
6	950	yes

Table 3: Timeline of water replacements in ambient conditions.

Time since first immersion (days)	pH immediately before replacement
1	6.5
6	9.5
15	not measured
39	6.5
69	6.0
130	5.5
133	not measured

Raman spectra were acquired using a Horiba LabRAM Soleil instrument. For each spectrum, we performed two accumulations of 3–5 s each, using a 532 nm laser running at 32 mW. Grating was set to 1800 and the hole size was 200 µm.

2.2 Low-temperature dissolution experiments

After all studies on the pristine high temperature experiments were complete, a second set of sectioned crucibles (Figure 2E–2H) was placed face up in a beaker and gently filled with 0.5 L of tap water. The water was replaced several times in increasing time gaps, and the pH was measured using a paper pH indicator (Table 3). The final water replacement after 130 days utilised deionised water.

After 133 days, the samples were removed from the beaker and dried in air for around two hours. Optical observation through binoculars revealed growth of crystalline material on top of the surface, and the samples were taken for observation in a Hitachi TM4000II environmental SEM (eSEM) that does not require any polishing or carbon coating. In order to confirm the crystalline material identity, we used the Raman method described above.

For a more thorough assessment of low temperature alteration processes, we repolished the experiments with sandpaper to flatten the surface, dried in a 120 °C oven, cleaned in an ultrasonic bath, and reimpregnated with epoxy. After a final polishing step down to 0.25 µm, the samples were examined using the FE-SEM as described earlier.

3 Results

3.1 High-temperature magmatic experiments

3.1.1 *Within the calcite stability field*

Experiments 1 to 4 were conducted within the calcite stability field in a surface pressure CO_2 atmosphere (<900 °C). The experimental products are dominated by calcite phenocrysts with typical sizes from 10–50 µm, consistent with previous work showing liquidus calcite in some synthetic natrocarbonatites [Watkinson and Wyllie 1971; Kjarsgaard et al. 1995; Lee and Wyllie 1996]. We qualitatively observed that calcite grain size increased with temperature (Figure 3A–3C), with 10–20 µm grains common in the 750 °C experiment (run 1; Figure 3A), whereas 50 µm grains are abundant in the 850 °C experiment (run 3; Figure 3C). The crystal shape is subhedral with tabular stubby prisms and strongly rounded dipyramidal terminations. Basal cross sections are likewise rounded, but some cases exhibit a very faint hexagonal shape [cf. Lee and Wyllie 1997]. Rounded calcite is typical for high temperature experimental studies [Lee and Wyllie 1996; Mitchell and Kjarsgaard 2008; Gittins and Mitchell 2023], and ours are no exception. Some calcite grains in the 750 °C experiment have cores with a darker BSE contrast, which we interpret as residual pure $CaCO_3$ from the starting materials (arrows in Figure 3A). No such cores are observed in the hotter runs. After CaO, the next abundant chemical component in calcite is SrO at 1.0 ± 0.2 wt.% (Table 4). In addition, low K_2O and Y_2O_3 contents, at or close to the detection limit of our EDS method, were found in many calcite grains.

Carbonatite liquids do not typically quench to glass, instead forming a dendritic intergrowth of carbonate minerals and other accessory phases. Accordingly, the matrix surrounding calcite mostly contains a mixed Na–Ca–K carbonate mineral (Figure 3, Table 5). This mineral is presumably nyerereite, but our mineral is more calcic than any other published nyerereite composition (Figure 4A). The Ca-rich character makes it compositionally closer to $Na_2Ca_2(CO_3)_3$ (shortite) than to end-member nyerereite at $Na_2Ca(CO_3)_2$ [also noted by Mitchell and Dawson 2021]. Although potassic shortites have been previously identified [Golovin et al. 2017b, and see "shortite?" field in Figure 4A], our Raman spectrum (Figure 5) does not agree with published Raman spectra for shortite, potassic or otherwise [Golovin et al. 2015; Káldos et al. 2015; Golovin et al. 2017a]. Instead of two distinct peaks in the carbonate region, we only find a single somewhat wider peak (Figure 5B), mostly consistent with known nyerereite Raman spectra [Golovin et al. 2017a; Berkesi et al. 2023]. Shortite is unstable at high temperatures, where it decomposes to nyerereite and calcite [Frankis and McKie 1973; Cooper et al. 1975]. To complicate things further, nyerereite may have different polymorphs at different temperatures (including zemkorite) with questionable preservation during quenching [Golovin et al. 2015; Christy et al. 2021]. It is possible that the high Ca contents of our phase stabilise a certain structure over another, but delving into this issue is beyond the scope of this project. Our compositions form the Ca–K-rich end of a compositional trend of Na–Ca–K-carbonates often referred to in the literature as "nyerereite", a trend distinct to analyses of coexisting Na–Ca–K-carbonates with a shortite-like composition [Figure 4A; e.g. Guzmics et al. 2011; Mitchell and Dawson 2021]. Consequently, we will simply refer to this carbonate as nyerereite*.

*Single crystal XRD measurements conducted after the acceptance of this paper indicate that this mineral may in fact be zemkorite and not

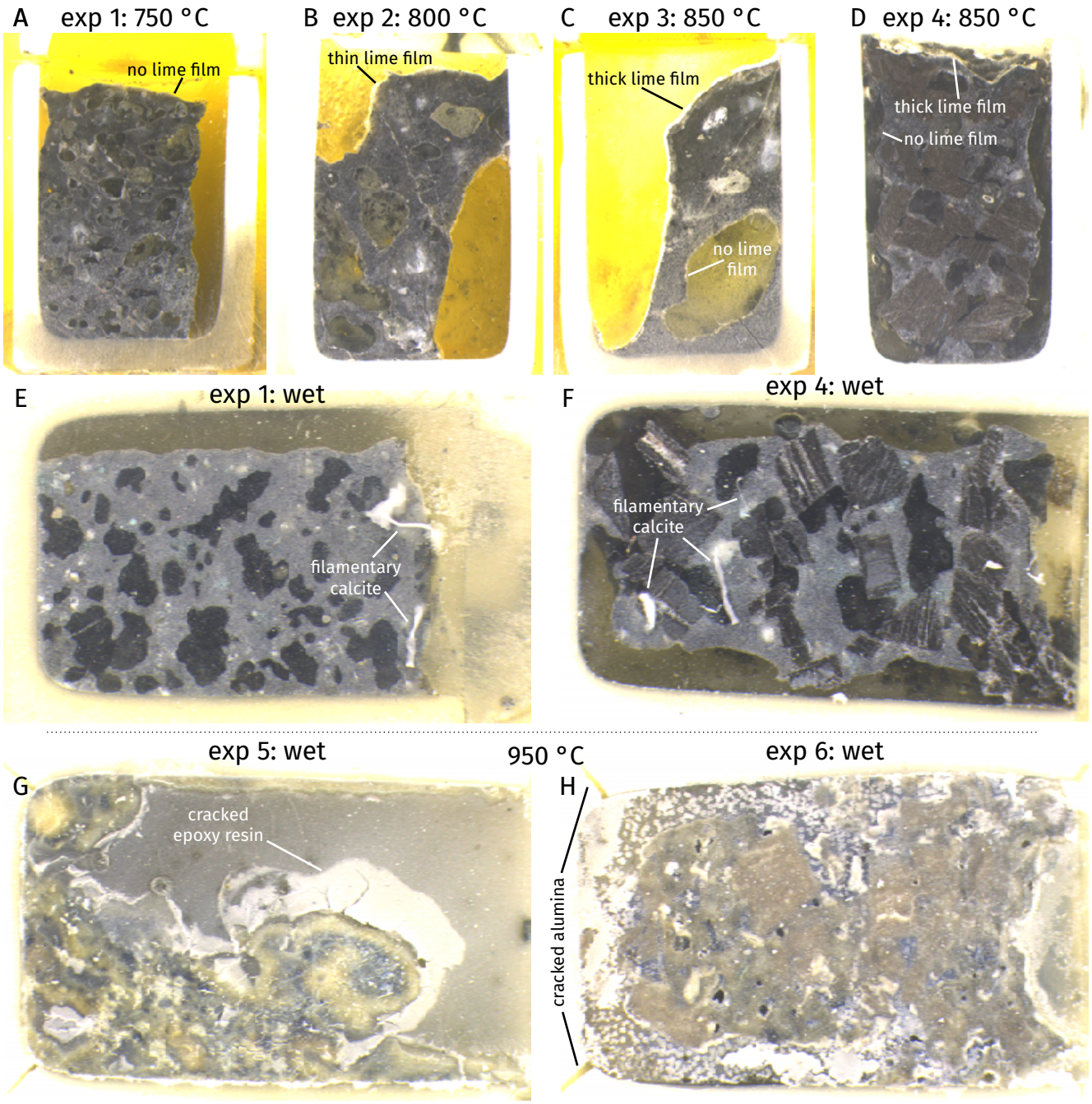

Figure 2: Reflected light images of sectioned alumina crucibles. [A–C] Surfaces of high temperature experiments taken within minutes of polishing. [D] Similar to previous, with calcite cleavage fragments in dark brown. [E–F] Polished surfaces after immersion in water. White patches and filamentary features are calcite structures that protrude above the samples up to about 1 mm to the direction of the camera. [G–H] Initially lime-rich experiments after immersion in water, showing substantial volumetric expansion demonstrated by cracked epoxy resin and alumina crucible walls. Recrystallised material protrudes above the polished surface up to about 1.5 mm. Note abundant spherical calcite.

Nyerereite occurs as elongated laths, which are more obvious in regions with lower abundance of calcite phenocrysts (e.g. Figure 3D–3F). Other than the major elements, it contains minor amounts of SrO (≈0.5 wt.%), P_2O_5 (≈0.5 wt.%), SO_3 (≈2.5 wt.%), and BaO (≈0.2 wt.%). In the lowest temperature experiment 750 °C, 1 atm), some nyerereite crystals are zoned with a darker BSE contrast in their cores whereas the rims are brighter due to elevated sulfate contents (Table 5, dashed ovals in Figure 3A, up to 18 wt.% SO_3). In all other experiments nyerereite grains have a homogenous BSE contrast. We interpret this to indicate that some nyerereite was an equilibrium mineral at 750 °C with additional nyerereite forming during rapid cooling upon removal from the furnace. In the hotter exper-

nyerereite. The two are isochemical polymoprhs and this has very little implications for the conclusions of the paper

Table 4: Compositions of calcite in wt.%. For experiment 3 at 850 °C, equilibrium phenocrysts are distinguished from elongated quench calcite. Secondary (2^{nd}) calcite spots were measured on BSE dark and light areas of grain in Figure 8D.

	750 °C	800 °C	850 °C (q.)	850 °C (eq. ph.)	2^{nd} dark	2^{nd} light
n	7	3	5	5	1	2
Na_2O	0.01	0.08	n.d.	0.00	0.38	0.25
P_2O_5	n.d.	n.d.	n.d.	0.00	0.82	0.91
K_2O*	0.12	0.09	0.16	0.11	0.13	0.11
CaO	51.30	51.57	51.51	51.25	51.51	50.41
SrO	1.07	0.79	0.97	0.82	0.56	0.82
Y_2O_3*	0.27	0.22	0.19	0.34	n.d.	0.13
BaO	n.d.	n.d.	0.17	n.d.	1.11	2.45
Total	52.87	52.97	53.10	52.58	54.51	55.06

n.d.—not detected; q.—quench calcite laths; eq. ph.—equilibrium calcite phenocrysts.
* K_2O and Y_2O_3 were often at the detection limit, and should be considered as qualitative estimates.

Table 5: Representative compositions of alkali carbonates in wt.%.

	750 °C nyerereite core	750 °C nyerereite rim	800 °C nyerereite	850 °C nyerereite	950 °C nyerereite	950 °C gregoryite
Na_2O	19.00	19.45	19.54	19.46	17.19	33.46
P_2O_5	0.57	0.71	0.55	0.51	0.56	2.58
SO_3	4.08	18.83	2.40	2.69	2.07	10.23
Cl	0.09	n.d.	0.12	0.10	0.03	n.d.
K_2O	6.88	6.47	7.94	7.80	8.76	3.03
CaO	27.28	24.75	26.94	26.38	26.43	7.96
SrO	0.38	0.40	0.45	0.48	1.80	0.88
BaO	0.28	n.d.	n.d.	0.15	0.46	0.70
Total	58.47	70.75	57.81	57.52	57.39	58.85

n.d.—not detected.

iments, we suggest that no nyerereite was stable at run temperature, and all nyerereite formed by crystallisation from the cooling carbonatite melt. This is supported by the presence interstices between nyerereite laths. They are composed of a very fine-grained intergrowths of various phases, occasionally symplectic, that are compositionally not too dissimilar to nyerereite, but contain substantial fluoride and chloride contents, with occasional barium-rich sections (Figure 3G). These textures are consistent with quench textures observed in experiments on carbonatites previously [Mitchell and Kjarsgaard 2008], from natural natrocarbonatites [Dawson et al. 1990], and from secondary calcite carbonatites [Keller and Zaitsev 2006; Zaitsev and Keller 2006; Zaitsev et al. 2008] from Oldoinyo Lengai and Tinderet [Zaitsev et al. 2013]. Rarely, gregoryite occurs between nyerereite laths.

The matrix contains ovoid patches of a Mg-rich and Na–K–Ca-bearing carbonate (Figure 3C, 3D). They are porous and compositionally heterogenous (as evident by their mottled BSE contrast). These Mg-rich patches contain minor contents of all other cations used in our experiments (Sr, P, S, and Ba, Table 6). They appear to have been solid phases at run temperatures as they truncate the growth of calcite phenocrysts

Table 6: Compositions of ovoid Mg-carbonate patches in wt.%.

	750 °C	850 °C	950 °C
F	2.10	0.90	n.d.
Na_2O	10.91	12.42	21.58
MgO	41.00	33.81	42.04
P_2O_5	0.36	0.37	1.08
SO_3	3.08	2.08	5.15
Cl	n.d.	0.73	n.d.
K_2O	4.17	5.18	2.24
CaO	15.99	17.26	5.67
MnO	0.18	0.47	n.d.
SrO	0.56	0.29	0.79
BaO	0.90	0.68	0.47
Total	77.31	72.55	79.34

n.d.—not detected.

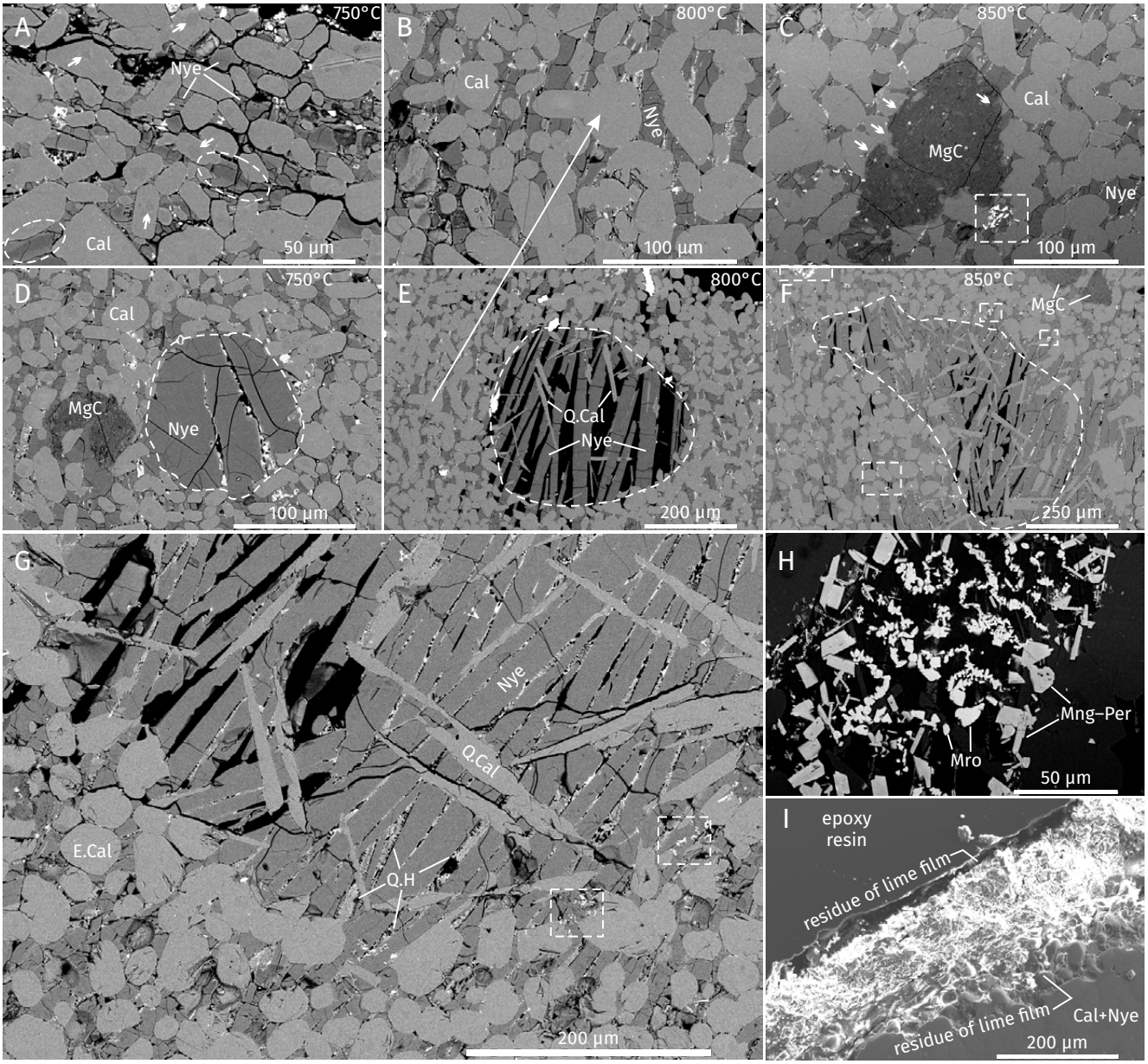

Figure 3: [A–C] BSE images of experiments 1–3 showing increasing calcite (Cal) grain size in mostly nyerereite (Nye) matrix. In [A], dark calcite cores are marked by arrows and dark nyerereite cores by dashed ovals. In [C], calcite terminated by Mg-carbonate (MgC) is marked by arrows, and oxide aggregates are marked by a dashed rectangle. [D–F] BSE images of melt pools marked with dashed outlines in experiments 1–3 showing increase of quench calcite (Q.Cal) proportions with temperature. [G] Close-up BSE image of a melt pool in experiment 3 with quench calcite distinguished from equilibrium calcite (E.Cal) and interstitial quench halides (Q.H.). [H] High contrast BSE image showing two different oxide minerals, marokite (Mro) and manganosite–periclase solid solution (Mng–Per). [I] SE image of experiment 3 showing residual lime and portlandite at the melt–atmosphere interface (now filled with epoxy resin).

(arrows in Figure 3C). However, we cannot conclusively determine that they were not Mg-rich immiscible carbonate melts, although we consider this option to be highly unlikely. The finding of a Mg-rich carbonate in our runs was surprising, because pure $MgCO_3$ decomposes to MgO at temperatures much lower than our run conditions. It was probably stabilised by its impure composition, and by having been immersed in carbonate melt.

Several phenocryst-free globular patches occur in our experiments (Table 7; Figure 3D–3F). They consist of the same matrix material observed elsewhere with nyerereite and halide-rich interstices (Figure 3G). In addition, these globules contain elongated calcite laths in the 800 and 850 °C experiments, which we interpret to crystallise directly from the melt during cooling—as distinguished from tabular calcite, present as an equilibrium phase alongside melt [Lee and Wyllie 1997]. The reason for the occurrence of these globules is uncertain,

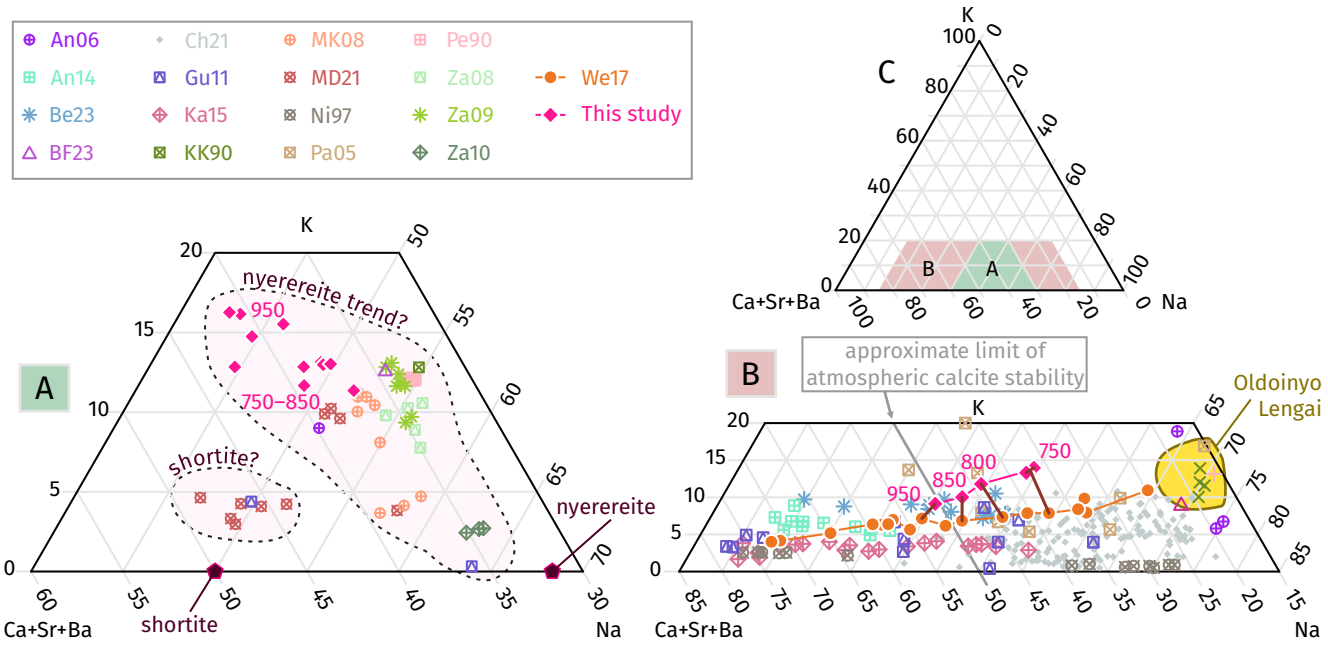

Figure 4: Ternary diagrams of K–Na–(Ca + Sr + Ba) on a molar basis. [A] Solid crystals. [B] Melt compositions. Melt compositions from experimental temperature series connected with similarly coloured lines. Brown lines connect our experiments with experiments at similar temperatures from Weidendorfer et al. [2017]. Dark grid line indicates approximate surface stability limit of calcite in a pure CO_2 atmosphere, such that hotter calcite-saturated liquids will decompose to lime upon eruption. [C] Full ternary range with shaded areas indicating plotted regions for the two previous panels. Data from Andreeva et al. [2006] (An06), Andreeva [2014] (An14), Baudouin and France [2023] (BF23), Berkesi et al. [2023] (Be23), Chayka et al. [2021] (Ch21), Guzmics et al. [2011] (Gu11), Káldos et al. [2015] (Ka15), Keller and Krafft [1990] (KK90), Mitchell and Kjarsgaard [2008] (MK08), Mitchell and Dawson [2021] (MD21), Nielsen et al. [1997] (Ni97), Panina [2005] (Pa05), Peterson [1990] (Pe90), Weidendorfer et al. [2017] (We17), Zaitsev et al. [2008] (Za08), Zaitsev et al. [2009] (Za09), and Zaitsev [2010] (Za10).

but we have no reason to believe that their melt composition was different to the melt that supported calcite phenocrysts. Some of the globules contain an abundance of empty space (now filled with epoxy resin; Figure 3E), suggesting they were hybrid melt–gas globules at high temperature, which would contribute to their lack of calcite phenocrysts. Calcium contents increase with temperature (Figure 4B), consistent with greater calcite proportions (Figure 3D–3F). Sulfate contents systematically decrease with temperature, with the 750 °C run containing around 5 wt.% of SO_3 whereas the hotter runs have ~2.5 wt.%. There are no sulfate phases in our experiments, so the 5 wt.% of the 750 °C run is consistent with our initial sulfate composition (5.02 wt.% SO_3; Table 1) and the sulfate required to form the sulfate rich nyerereite cores. This indicates a potential and unexpected loss of sulfate as gas, despite the overall refractory nature of sulfates in our run conditions and short duration of only two hours.

A small prismatic oxide mineral with a Mn:Ca ratio of about 2:1 occurs in aggregates throughout the experiments (dashed rectangles in Figure 3). The only known mineral consistent with our analysis is marokite ($CaMn_2O_4$) in which Mn is trivalent. We found that marokite was the only phase containing La detectable by EDS. Marokite imparts a dark, almost black, colour to the solidified lavas (see crucible interior in Figure 1). Preliminary experiments in which marokite was concentrated only in certain layers showed that marokite-free lavas were teal. This was also evident in the teal spillage from some experiments (e.g. in the bottom of the bucket in Figure 1). Due to the non-existence of marokite in natural carbonatites and the lack of La in any of the other phases, they will not be discussed further. Marokite is often associated with a calcic manganosite–periclase solid solution (Figure 3H) with Mn:Mg:Ca contents of about 65:30:5, containing Mn^{2+} (as opposed to Mn^{3+} in marokite). The coexistence of Mn^{2+} and Mn^{3+} indicates that oxygen fugacity was probably around the MnO–Mn_3O_4 oxygen buffer, which lies close to the MH buffer [O'Neill and Pownceby 1993].

In the 800 and 850 °C experiments (2–4), a thin film of lime was observed in the melt–atmosphere interface (Figures 2A–2D, 3I). We interpret this as the decomposition product of the $CaCO_3$ component in the melt when taken out of the pure CO_2 atmosphere inside the furnace to the ambient air which only contained around 415 ppm of CO_2 at the time of the experiments. This film was marginally thicker in the higher 850 °C experiment due to the slightly longer time it took to cool below the decomposition temperature of calcite in air (roughly 500–550 °C).

Experiment 4 was run at 850 °C and contained cleavage fragments of calcite (Figure 2D). Overall, the cleavage fragments remained intact with minor melt infiltration along cleavage planes. The surrounding matrix contained an identical assemblage to experiment 3, with rounded calcite phe-

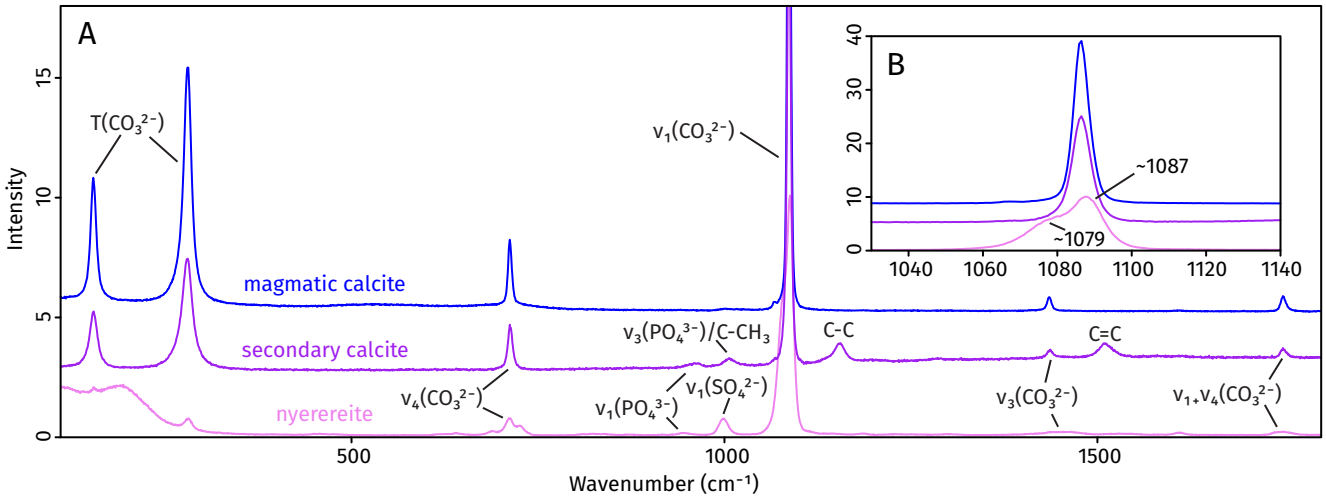

Figure 5: [A] Raman spectra of nyerereite (pink), secondary calcite (purple), and primary calcite (blue). [B] Magnification of the $\nu_1(CO_3^{2-})$ region. Primary calcite results in a typical clean calcite spectrum. Secondary calcite contains additional phosphate peaks, consistent with its minor P_2O_5 contents. Additional peaks indicate some organic material. It is unclear whether this organic material is part of the sample, introduced (perhaps bacterially) during dissolution experiments, or whether it is contamination introduced during polishing owing to the porous nature of secondary calcite. Nyerereite contains phosphate and sulfate peaks, consistent with its minor element composition. The $\nu_1(CO_3^{2-})$ region of nyerereite contains two poorly defined bands, consistent with its impure composition and potential low crystallinity derived from its formation during quench. Interpretation of Raman spectra guided by Hernanz et al. [2008], Golovin et al. [2017a], Golovin et al. [2015], Káldos et al. [2015], and Berkesi et al. [2023].

nocrysts and a nyerereite-dominated quenched melt phase (Figure 2D). Sharp corners in contact with the melt were recrystallised into a finer grained aggregate of rounded calcite crystals with a similar shape to phenocrysts (Figure 6). In places where the melt was absent or only consisted of a very thin film coating the cleavage fragments, this recrystallisation was minor to non-existing (Figure 6).

3.1.2 *Above calcite decomposition temperature*

No calcite was expected in experiments 5 and 6, conducted at 950 °C, higher than the calcite decomposition temperature of ~900 °C [Galan et al. 2012; Karunadasa et al. 2019]. Instead of calcite, phenocrysts were amoeboid lime (Figure 7A). Some lime contained patches with darker BSE contrast and accordingly lower analytical totals of 65–70 wt.%. These totals are higher than calcite (typically <55 wt.%) and it is unclear whether this is partly decarbonated calcite, intergrown on a nanoscale with lime, rapid rehydration of lime to portlandite, or something else. Unfortunately, this material proved unstable and was altered to portlandite dust within days before we had the opportunity to examine it with additional methods (e.g. Raman spectroscopy).

Calcite rhombs were completely decomposed to lime and penetrated by natrocarbonatite melt (now appearing mostly as nyerereite). These lime–nyerereite domains retain the overall outline of the decomposed calcite rhombs (Figure 7B). The former liquid matrix is similar to the previous experiments and dominated by nyerereite, with occasional oxide minerals and fine-scale dendritic intergrowths of halide-rich material (Figure 7C). Nyerereite is substantially richer in SrO than previous experiments, probably because the lack of calcite to sequester Sr (Table 5). Gregoryite is more common in these runs, often occurring between nyerereite laths, and contained elevated amounts of many elements other than Na (Table 5; Figure 7A).

We found small patches of wollastonite in some parts of the capsule, which we interpret to result from the reaction of the melt with any silicate minerals which were accidentally included with the calcite rhombs (Figure 7C). Interestingly,

Table 7: Compositions of melt pools in wt.%.

	750 °C[a]	750 °C[a]	800 °C[b]	850 °C	950 °C
Na_2O	18.77	17.80	16.53	15.66	14.59
MgO	0.08	n.d.	n.d.	n.d.	0.09
SiO_2	0.18	0.24	0.82	0.20	0.24
P_2O_5	0.54	0.42	0.44	0.46	0.24
SO_3	4.46	5.69	2.47	2.43	2.32
K_2O	8.07	7.37	6.68	5.54	5.02
CaO	24.73	24.38	29.24	30.36	32.18
SrO	0.58	0.55	0.50	0.65	1.11
BaO	0.44	0.81	0.32	0.69	0.93
F	0.29	1.22	n.d.	1.36	n.d.
Cl	n.d.	0.61	0.40	0.18	n.d.
Total	57.83	57.26	57.00	55.98	56.72

[a] Two different melt pools analysed for experiment 1.
[b] Raw data had low totals stemming from large epoxy-filled cavities in the rastered area, and was normalised to 57 wt.% to standardise it with the other measurements.
n.d.—not detected.

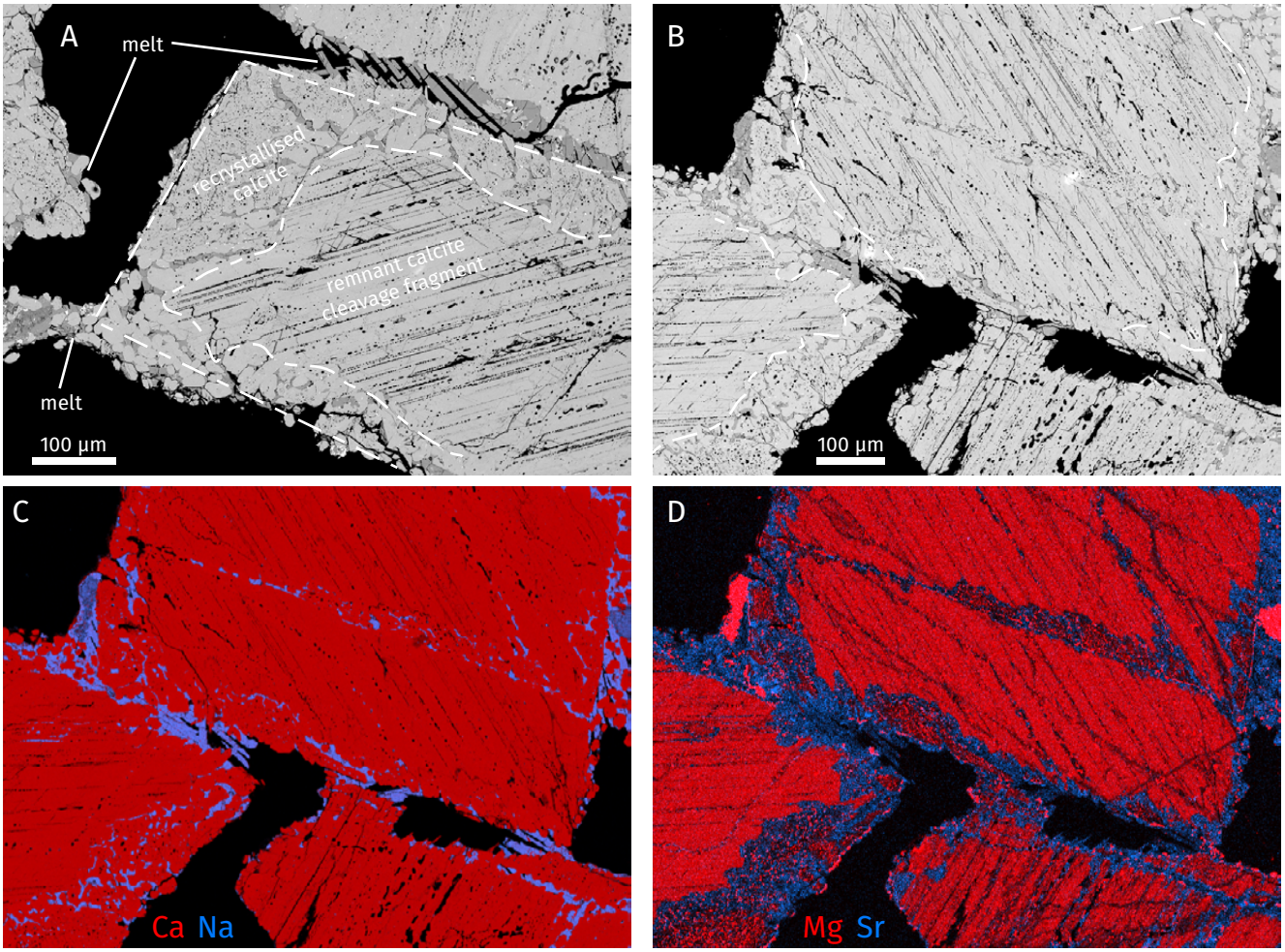

Figure 6: [A, B] BSE images of calcite rhombs from experiment 4, where the rims are surrounded by a thin film of natrocarbonatite melt. The calcite rhombs contain an unmodified core, mantled by a recrystallised zone which contains small rounded calcite crystals with minor interstitial melt, annotated by the dashed lines. The unmodified cores are distinguished from the recrystallised mantles by a slightly darker BSE contract owing to minor Mg contents whereas newly crystallised calcite is brighter as it contains minor Sr. [C] A WDS map of [A] showing the Ca in red and Na in blue, distinguishing calcite from sodic melt. [D] A WDS map of the same region, showing original Mg-rich calcite rhombs in red and recrystallised Sr-rich calcite in blue.

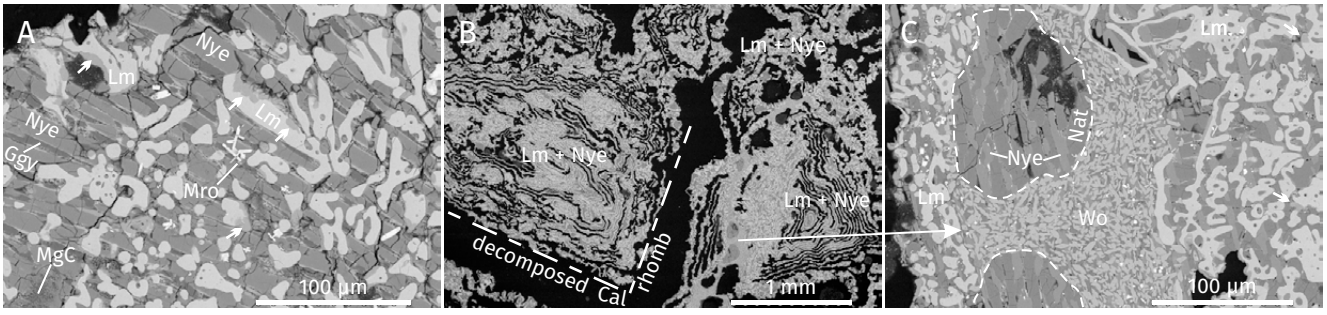

Figure 7: BSE images. [A] Experiment 5 with lime (Lm) in a matrix of nyerereite and gregoryite (Ggy). Patches of darker BSE contrast are shown with arrows. [B] Experiment 6 with decomposed calcite rhombs, now dominated by lime with interstitial nyerereite indicating melt infiltration after volume loss. [C] A closeup of [B] showing a melt pool with small-scale crystallisation of wollastonite (Wo) forming after unplanned silica contamination.

the melt pool contains only traces of SiO_2, providing further support to the negligible silica solubility in carbonatite melts at crustal conditions [see discussion on antiskarns, Anenburg and Guzmics 2023; Anenburg and Walters 2024].

3.2 Low-temperature dissolution experiments

After immersion in water for roughly four months, almost all nyerereite dissolved (Figure 8A, 8B) apart from minor residues which could only be accessed after repolishing and exposure of fresh surfaces (Figure 8C, 8D). Previous dissolution attempts only lasted 24 h, in which most nyerereite was retained, demonstrating the benefit of running months-long experiments [Keller and Krafft 1990]. Any halide-rich phases interstitial to nyerereite were completely gone, except fluorite. All original calcite, regardless of genesis (cleavage fragments, phenocrysts, or quench laths), remained intact (Figure 8A, 8B). Raman spectroscopy and EDS analyses confirmed substantial growth of new calcite (Table 4; Figure 5), filling in cavities formed by dissolution of nyerereite. Rare examples of residual nyerereite contain rounded dissolution holes filled with euhedral calcite (Figure 8C, similar to calcite–shortite relationships observed by Zaitsev et al. [2008]). This nyerereite is porous with patchy and fine-scale zone indicating Na-loss (Figure 8D). Most newly-crystallised calcite has a euhedral trigonal shape with grain sizes up to 50 µm. We found occasional aggregates of larger calcite crystals with somewhat rounded rhombohedral shapes (Figure 8E, 8F). Rarely, these aggregates serve as roots for calcite filaments or tubes growing upwards from the surface or the sample up to a height of 1 mm (Figures 2E, 2F, 8E, 8F). This filamentary tubular calcite has conspicuous growth steps, and occasionally forms a closed loop where it contacts the surface of the sample at its other end (Figure 8E). This new calcite is often porous and compositionally heterogeneous, with the brightest BSE zones reaching up to 2.5 wt.% BaO (Table 4; Figure 8D). In addition, this new calcite contains up to 1 wt.% P_2O_5, 0.8 wt.% SrO, 0.4 wt.% Na_2O, and 0.2 wt.% K_2O (Table 4). It is unknown whether these elements are present in the calcite solid solution, or whether they occur as discrete nano-scale phases which could not be resolved using our methods (with a similar question raised by Zaitsev et al. [2013]). Raman spectroscopy suggests some incorporation of organic material (Figure 5), but confirmation this requires further investigation beyond the scope of this manuscript. Often, calcite crystals are coated by fluorite or baryte. Baryte also occurs as ~1 µm inclusions in calcite (Figure 8A, 8D).

Experimental runs 5 and 6 (950 °C) experienced substantial swelling with a sufficient force to crack the alumina crucible and epoxy resin (Figure 2E, 2F). Here, calcite often occurs as spherical aggregates, themselves composed of many subspherical aggregates of rounded subhedral calcite (Figure 8G). In addition to calcite, euhedral portlandite prisms occur in some of the larger dissolution cavities, either as isolated crystals (Figure 8H) or as rounded aggregates (Figure 8I).

We acknowledge a limitation in our study whereby these dissolution and recrystallisation results are probably dependent on various conditions such as wetting and drying cycles, temperature, groundwater chemistry, etc. Natural dissolution of natrocarbonatites progresses in a more complex way than simple immersion in water, with formation of several intermediate minerals such as shortite, pirssonite, gaylussite, or trona [Dawson et al. 1987; Hay 1989; Zaitsev and Keller 2006; Zaitsev et al. 2008]. These minerals are water-soluble and form in nature owing to incomplete wetting–drying cycles. In our experiments, these water-soluble minerals did not form because of continuous water immersion. Nonetheless, we believe our results closely represent the end result of aqueous alteration of natrocarbonatites.

4 Discussion

4.1 Calcite morphology in extrusive carbonatite systems

Many carbonatites of alleged extrusive origin contain coexisting calcite of different textures and compositions. Often, calcite phenocrysts are surrounded by a calcite-dominated matrix, typically with abundant iron oxides [Dawson 1964b; Le Bas and Dixon 1965; Keller 1981; Deans and Roberts 1984; Woolley et al. 1991; Campeny et al. 2014]. Calcite crystals of all associations exhibit many different crystal shapes, described as fibrous, euhedral (presumably rhombohedral), anhedral, and platy [Deans and Roberts 1984; Keller 1989; Barker 2007; Zaitsev et al. 2013; Mitchell and Dawson 2021]. Of interest is the description of Kerimasi by Mariano and Roeder [1983] who suggest that lavas were initially natrocarbonatites with calcite phenocrysts, and were later altered to produce an almost monomineralic calcite rock. They show a groundmass of extremely fine-grained euhedral calcite (5 µm) that presumably replaced nyerereite, and large tabular and elongated calcite crystals. They also show several tabular calcite crystals with somewhat rounded skeletal-like elongated appendages [also observed elsewhere, see Turner 1988; Rosatelli et al. 2003]. Although Mariano and Roeder [1983] do not elaborate on this texture, the resemblance to our quench calcite (Figure 3) is remarkable. This hypothesis received additional support with Zaitsev [2010] discovering that magnetite in these rocks contains inclusions of nyerereite, itself sometimes altered to calcite. Evidently, the Kerimasi natrocarbonatites differed from the better known Oldoinyo Lengai lavas by being calcite-saturated [Guzmics et al. 2011] and therefore with a Ca-richer carbonatite melt that formed additional calcite as it cooled (although calcite-saturated natrocarbonatites probably existed in pre-modern eruptions of Oldoinyo Lengai, see Hay [1989]). Next, fine grained calcite rhombohedra formed upon aqueous alteration of nyerereite (similar to textures in Figure 7). Essentially, our experiments faithfully recreate currently observed textures at Kerimasi.

In some cases, calcite-dominated extrusive carbonatites have been interpreted as cemented and recrystallisation-hardened ashes that rained down during explosive eruptions [Dawson 1964a; b; Campeny et al. 2014]. This is supported by previous observations of carbonate ash in carbonatite volcanoes. However, the only ash to have been witnessed during eruption was the natrocarbonatite ash at Oldoinyo Lengai, which contained no calcite [Hobley 1918; Woolley 2021]. All other accounts of carbonatite ash were formulated after the event, and assertions for the unaltered nature of said ashes are questionable [e.g. von Knorring and du Bois 1961; Keller

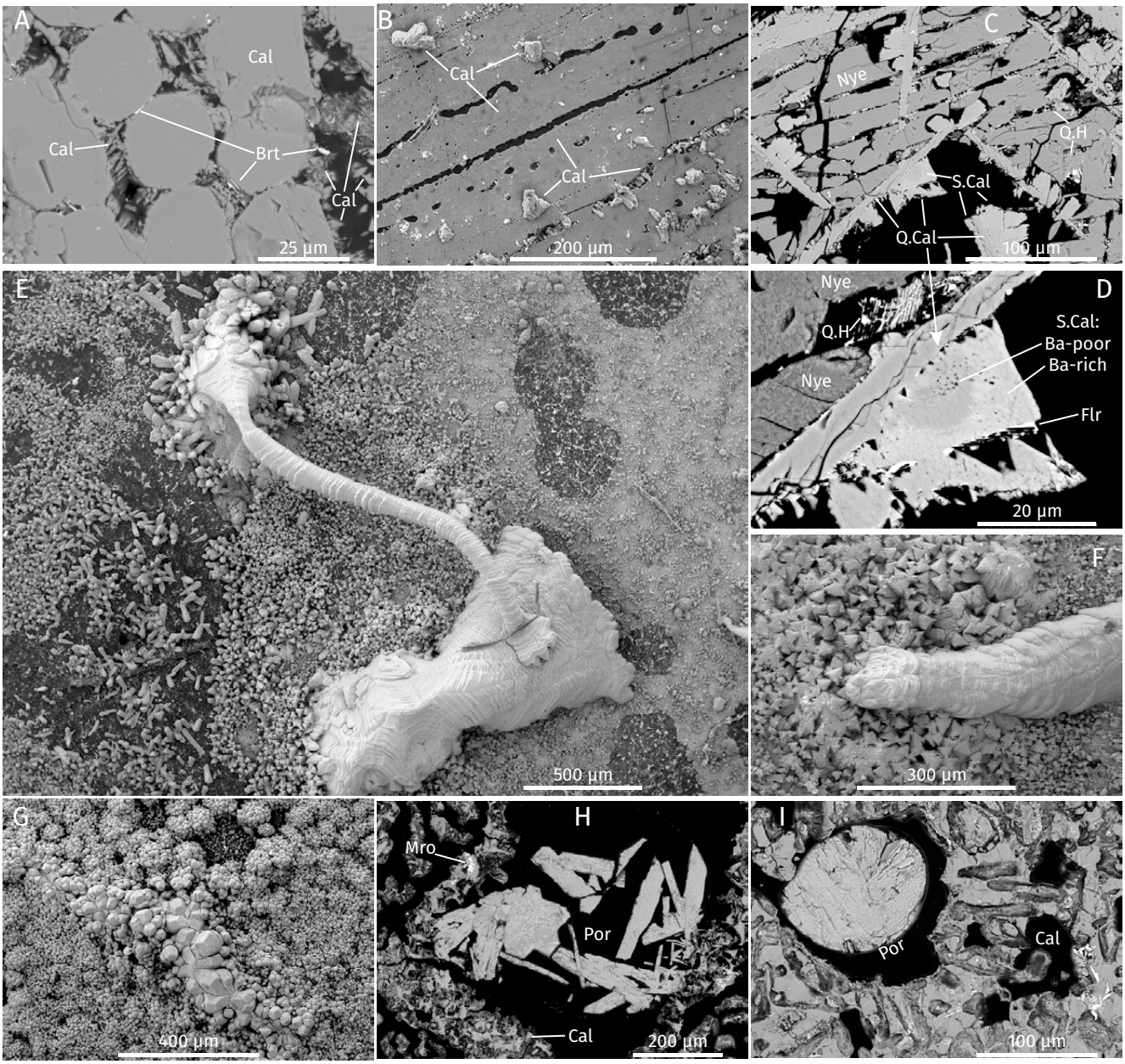

Figure 8: [A] BSE image of calcite phenocrysts with formerly nyerereite-filled interstices replaced by secondary calcite and baryte (Brt). [B] SE eSEM image of a calcite rhomb, with cleavage planes infiltrated by melt now replaced to calcite. Additional calcite is growing on the surface. [C] BSE image of a partly-preserved melt pool exposed by deep polishing showing secondary calcite (S.Cal) growing on quench calcite laths, replacing nyerereite. [D] A higher contrast close-up of [C] showing zoning euhedral calcite with compositional zoning, and patchy zoning in nyerereite. [E–G] SE eSEM images showing filamentary and rounded aggregates of calcite growing on the polished surfaces of experiments 1, 3, and 5, respectively. Everything in the images is calcite, except the darker epoxy patches in the substrate. [H–I] Portlandite replacing lime in the 950 °C experiments, in a matrix of mostly calcite.

1981; Barker and Nixon 1989; Eby et al. 2009; Rosatelli et al. 2010; Toscani et al. 2020]. We stress that ashes cannot be solidified calcite that was liquid during the eruption owing to its refractory nature. At Kaiserstuhl, Keller [1981] argues that droplet-like lapilli, composed primarily of calcite with no other carbonates, represent calcitic melt that was erupted as a liquid. Calcite in the lapilli consists of elongated calcite laths in a matrix of fine-grained calcite. We agree with the interpretation of the calcite laths as igneous crystallisation from a liquid—they look remarkably like the elongated quench calcite produced in our experiments. However, the calcite matrix cannot represent liquid calcite. Our experiments put a limit on the amount of $CaCO_3$ that can be dissolved in a natrocarbonatite melt (Figure 4B, see below), such that any additional $CaCO_3$ simply adds more solid calcite, and does not shift the liquid to more calcic compositions. That the melt had initially

been alkaline is supported by abundance of alkaline melt and fluid inclusions from Kaiserstuhl [Walter et al. 2021]. Even if the melt was alkali-poor and still liquid at a shallow depth of several tens of metres [as proposed by Wyllie and Tuttle 1962], calcitic liquids would solidify immediately upon eruption and not maintain their droplet shape (according to cooling models by Capaccioni and Cuccoli [2005]), particularly for the duration required for droplets to land back at the surface (as hypothesised by Keller [1981]). Instead, we proffer that the lapilli were calcite-saturated natrocarbonatite melts that crystallised to elongated quench calcite in a matrix of nyerereite. Nyerereite was then inevitably replaced by fine-grained calcite during aqueous alteration. This is supported by isotopic studies on the Kaiserstuhl lapilli showing the primary nature of the calcite phenocrysts, but secondary nature of the groundmass calcite [Hubberten et al. 1988]. Keller [1981] claims that the vesicular nature of the lapilli indicates that replacement could not have occurred because any introduction of Ca would result in calcite filling in cavities. Conversely, our experimental results indicate that Ca introduction is not required, as it is supplied by the $CaCO_3$ component in the nyerereite solid solution, all the more so with Ca-rich nyerereite expected in calcite-saturated environments (Figure 4A). The porous nature of the Kaiserstuhl lapilli is consistent with volume loss, as expected by dissolution. The overall droplet shape of lapilli stones need not be erased during alteration, with abundant examples of nyerereite phenocrysts retaining their crystal shape upon replacement to calcite [Hay 1983; Deans and Roberts 1984; Clarke and Roberts 1986; Zaitsev and Keller 2006]. This possibility was also noted by Dawson et al. [1987] and Mariano and Roeder [1983]. Natural nyerereite has been observed to alter to pirssonite and gaylussite [Zaitsev and Keller 2006], resulting in a volume increase. In many extrusive calcite carbonatites there is good preservation of magmatic textures, indicating no volume increase. This led some to suggest that calcite cannot pseudomorph nyerereite as original textures will be destroyed [Gittins and Jago 1991; Gittins and Harmer 1997; Mitchell and Dawson 2021]. However, our results indicate that immersion in water leads to dissolution of nyerereite and replacement to calcite without an intermediate pirssonite stage (Figure 7C), solving the volume increase paradox (the paradox may not even exist, see Keller and Zaitsev [2006]). Furthermore, Zaitsev and Keller [2006] demonstrate clear replacement of nyerereite by fine-grained euhedral calcite in their study of Oldoinyo Lengai. The calcite is often zoned and appears in contact with outlines of nyerereite ghosts. Zaitsev and Keller [2006] do not elaborate on which elements cause zoning, but their data tables indicate highly variable BaO contents, and the resemblance to our secondary calcite is striking (Table 4). We only observe volume increase in cases where calcite decomposed to lime at temperatures greater than 900 °C, and then rehydrated (Figures 2G, 2H, 8G).

We suggest the alternative hypothesis that most, if not all, fine-grained calcite that occurs as cements and other matrix materials is the residue of dissolved Ca-bearing alkali carbonates, as suggested before [Hay 1983; Mariano and Roeder 1983; Deans and Roberts 1984; Bambi et al. 2012; Campeny et al. 2015]. Nyerereite in calcite-saturated natrocarbonatites is richer in Ca, providing more material for secondary calcite formation (Figure 4A). In a detailed study of the Tinderet volcano, Deans and Roberts [1984] provided the first compelling and holistic account for calcification of natrocarbonatite, further corroborated by Zaitsev et al. [2013]. They identify mostly intact semi rounded tabular calcite phenocrysts or antecrysts, and calcified groundmass which they interpret as replacement of often quenched dendritic nyerereite. Similarly, Mariano and Roeder [1983] and Hay [1983] in their study of Kerimasi, identify tabular clean primary calcite in a matrix of dirty fine-grained calcite that formed as a replacement of nyerereite. We agree with this interpretation, and it is well supported by our experiments (Table 4, Figure 8). Additionally, Deans and Roberts [1984] identify coarser grained calcite with the same characteristics of the groundmass replacement calcite, which they interpret as pseudomorphs after nyerereite phenocrysts. Although in our experiments we did not form any clear nyerereite phenocrysts (whether the nyerereite cores in run 1 at 750 °C are true phenocrysts is speculative), we have no reason to believe that the Deans and Roberts [1984] interpretation is wrong, given similar findings by Zaitsev and Keller [2006]. We find that any pre-existing calcite is unharmed by the alteration process (Figure 8A), whereas nyerereite has the clear propensity to transform to calcite (Figure 8B, 8C). Therefore, we agree that if coarse grained calcite looks similar to other clearly finer-grained calcite pseudomorphs—in terms of texture and composition—then it is indeed replacing nyerereite. Our demonstration of alteration of nyerereite to calcite whilst in the presence of preexisting calcite phenocrysts is crucial (Figure 8). Too often, the fact that both textural varieties of calcite can coexist has been overlooked, leading to somewhat staunch claims on both side of the debate [e.g. Gittins and Harmer 1997; Campeny et al. 2015].

4.1.1 *Eruptions hotter than calcite decomposition temperature*

The above discussion concerned lavas erupted within the calcite stability field. However, Ca-richer carbonatite melts are possible in higher temperatures or pressures (Figure 4B). Once erupted, the fate of these compositions is constrained by calcite stability at atmospheric pressures. As demonstrated by experiments 5 and 6, calcite would decompose to lime with substantial volume reduction (Figure 7B). A calcic natrocarbonatite melt will intrude newly-formed holes in decomposed calcite, which will solidify primarily to calcite. The melt itself can also decompose upon expose to the atmosphere, forming additional lime (Figure 3I). It is unknown how rapid the decomposition is, because dynamic changes in gas composition and temperature are difficult to recreate in our experimental setup. However, formation of lime films indicates that decomposition can occur in seconds. This is supported by Galan et al. [2012] who demonstrated substantial $CaCO_3$ decomposition occurring in under a minute at temperatures of ~950 °C. A natural rock will likely contain fine-scale intergrowths of partly decomposed calcite, lime, and nyerereite (Figure 7B). Alteration of this assemblage will lead to volume expansion by hydration of lime to portlandite, and finally a perplexing calcite-dominated rock with no obvious calcite phenocrysts or evidence for nyerereite replacement (Figure 8H, 8I).

Curiously, Hay [1978] described calcite globules from the Laetolil beds that he interpreted as replacement of solidified natrocarbonatite droplets. Hay [1983] later revised the interpretation to that of gas bubbles filled with late calcite. We note that these calcite globules look remarkably like the spherical calcite aggregates observed in our 950 °C experiments (runs 5 and 6, Figure 2H). The Hay [1978] calcite globules are associated with melilite, which is typically a higher temperature mineral. We suggest that perhaps those natrocarbonatite lavas erupted at a temperature higher than the calcite decomposition point at roughly 900 °C, or close to it, such that formation of at least some lime formed and subsequently altered to spherical calcite aggregates.

4.1.2 *Rounded calcite*

A decades-long debate concerned whether round calcite globules in experiments and natural rocks represent anhedral (or at least non-rhombic) solid calcite crystals, or solidified liquid calcite liquid [e.g. Pirajno and Yu 2022]. Gittins and Mitchell [2023] reviewed the history of this debate and came to the conclusion that round calcite is not solidified liquid, but instead it is solid calcite. Our findings support this view, with round calcite being the dominant morphology in our experiments. Only some grains are elongated and approach "tabular" shape (Figure 3). Moreover, our rhomb-bearing experiments show that even if classically-shaped euhedral calcite rhombs are introduced into a carbonatite melt, they destabilise and transform into the rounded shape (Figure 6). Gittins and Mitchell [2023] raised the question of why experimental calcite is always round whereas natural calcite is not. In our experiments we find that only equilibrium calcite is rounded (Figure 3A–3C). Calcite formed during quench is highly elongated (Figure 3E–3G). We extend this to natural systems where lavas are slowly cooled rather than quenched, leading to the typical morphology of somewhat rounded, but tabular crystals.

Calcite morphology can also change at low temperatures. During subsequent alteration of natrocarbonatites, $CaCO_3$ residues from nyerereite can lead to secondary calcite overgrowths on primary round calcite, straightening some of the crystal faces making them less rounded (e.g. Figure 8D). Rounded calcite aggregates can also form by carbonation of lime or portlandite.

We note that this discussion is mostly relevant for monomineralic calcite globules. Rounded calcite globules containing other carbonatite-typical minerals probably were liquid carbonatite droplets [Rosatelli et al. 2003; Zaitsev et al. 2003; Eby et al. 2009]. We emphasise that these droplets likely contained nyerereite, which is now all transformed to calcite.

4.2 Compositional trends

4.2.1 *Carbonatite melts*

There are great uncertainties on compositions of natural carbonatite melts. Published carbonatite melt compositions are usually derived from homogenised melt inclusion data, and cover most of the compositional range from Ca-rich (but nonetheless alkaline) to Na-rich Oldoinyo Lengai type natrocarbonatites. Despite issues with carbonatite melt inclusion data (such as lack of quenched glasses, volatile or alkali loss, and post entrapment modification), we consider the compositional range to provide a semi-quantitative estimate of natural liquids. Our liquid compositions mostly agree with published data (Figure 4B). Most useful is the comparison to the Weidendorfer et al. [2017] experiments, who show the only systematic experimental study covering almost the entire range of natural melt compositions. Our natrocarbonatite compositions follow their experiment at equivalent temperatures (albeit at slightly higher K_2O contents; Figure 4B). This indicates that between 1 bar and 1 kbar, there is no appreciable pressure effect. Weidendorfer et al. [2017] also demonstrated liquidus calcite down to about 630 °C, lower than our lowest temperature run at 750 °C.

Since these melts are calcite-saturated, the natrocarbonatite lavas cannot contain any more $CaCO_3$. If the entire system is more calcic, the implication is simply a higher proportion of solid calcite phenocrysts. The surface pressure calcite stability limit of ~900 °C in a carbon dioxide atmosphere, and lower in more realistic atmospheric compositions, prevents the formation of lava flows with Ca contents higher than indicated by the dark grey grid line on Figure 4B. Eruption of these compositions at >900 °C will lead to a lava flow with unstable calcite phenocrysts, and higher $CaCO_3$ than possible in surface conditions calcite-saturated melt. Thus, in rapid cooling the excess $CaCO_3$ will immediately solidify to calcite whereas in slow cooling calcite will decompose to lime, and additional lime crystals will form in the lava.

4.2.2 *Calcite*

The Ba-rich composition of our secondary calcite (Table 4, Figure 8D) is consistent with natural observations of calcite suggested to replace nyerereite, where its BaO contents are greater than BaO in associated calcite phenocrysts, if present [Hay 1983]. Zaitsev and Keller [2006] and Keller and Zaitsev [2006] show convincing evidence of secondary calcite with high SrO, BaO, K_2O, and P_2O_5, among other elements. Intergranular calcite from presumed altered natrocarbonatite dykes from Oldoinyo Lengai likewise show high BaO of up to about 1.5 wt.% [Dawson 1993; but not without controversy, Gittins and Harmer 1997]. Elevated K_2O, Na_2O, and P_2O_5 in calcite understood to replace nyerereite is also observed at Tinderet, in contrast to tabular calcite phenocrysts that are rich primarily in SrO and nothing else [Deans and Roberts 1984; Zaitsev et al. 2013], in agreement with our experimental results (Table 4; Figure 8D). The altered natrocarbonatites described by Dawson [1993] also contain pure Sr-bearing calcite, suggesting their magmatic origin alongside secondary calcite. Zaitsev [2010] and Zaitsev et al. [2013] similarly describe presumably phenocrystic pure Sr-calcite, and a groundmass of impure and zoned calcite. Zaitsev [2010] writes about the banded nature of this groundmass calcite, and whether it indicates alteration of both nyerereite and gregoryite, but our experiments indicate that secondary calcite can be zoned (or “banded”) by alteration of nyerereite alone. Similar relationships are shown for the Rangwa Complex, where phenocryst calcite is typically purer than fine-grained matrix calcite (although with much variability, and without comment by Rosatelli et al. [2003] on whether alteration of nyerereite is implicated in its genesis).

Although the textural type of this calcite is not specified by Dawson [1993], he differentiates it from secondary calcite (the Ba-rich "intergranular calcite" mentioned above), implying that it is primary tabular calcite. The overall higher SrO contents of phenocrystic calcite relative to secondary calcite have been observed elsewhere [Barker and Nixon 1989]. Curiously, the high BaO and SrO of calcite from Rockeskyll (Eifel) were used to interpret it as magmatic because presumably low temperature calcite should reject Sr and Ba [Riley et al. 1996; also see a recent perspective by Stoppa et al. 2023]. Our experiments clearly show the contrary, with higher Sr and Ba in calcite replacement of nyerereite compared to calcite phenocrysts. Riley et al. [1996] also show elevated P_2O_5 and K_2O contents in their calcite, further supporting our suggested alteration model (Table 4). Rapprich et al. [2024] documented Na-rich calcite rims and groundmass in lapilli from Kaiserstuhl, which they likewise used to argue against calcification, but our results indicate the opposite: sodic calcite is consistent with replacement of a nyerereite and indicate the former presence of natrocarbonatite lava (Table 4). Similar calcite compositions are described by Innocenzi et al. [2024] which they interpret as evidence for primary calcite, but our results indicate that their composition is more consistent with a secondary origin by alteration.

5 Implications for carbonatite lava compositions

Historically, the calcic composition of many extrusive carbonatites, together with the preservation of primary igneous textures, led to the widespread acceptance that many lavas were dominated by the liquid calcite component [Bailey 1993]. Kogarko et al. [1991], for example, asserted that "*calcium carbonate liquids undoubtedly exist, having been extruded as lavas and tuffs…*". This view has persisted in the literature, with claims that calcic carbonatite liquids can flow on the surface persisting to recent times [Mourão et al. 2010; Toscani et al. 2020]. Nonetheless, the notion that extrusive calcite carbonatites represent altered natrocarbonatites was not fully rejected (with Gittins and Harmer [1997] referring to this group as "calcitizers").

Our experiments indicate that the lava composition cannot exceed a certain amount of $CaCO_3$. Once a threshold is achieved, additional $CaCO_3$ merely adds more solid calcite (Figure 4B). Our compilation of carbonatite melt compositions supports this, showing that natural melts exist along a Na–Ca continuum with variable minor K, but never close to pure $CaCO_3$ compositions (Figure 4B). Whilst we have no objection to abundant phenocrystic calcite carried in natrocarbonatite lavas [e.g. Gittins and Jago 1991; Mitchell and Dawson 2021], we find no evidence to support that the liquid itself is anywhere near calcite composition. Calcitic carbonatite melts can exist underground at depths of just several tens of metres, but this requires sufficient dissolved H_2O. Water solubility in natural-like carbonatite melt compositions is negligible at surface pressures [Keppler 2003; Jacobson et al. 2020]. This indicates that any erupted calcitic liquid would crystallise immediately upon evaporation of its contained water. Moreover, although Ca-dominated compositions have been demonstrated in experiments, whether they exist in nature is open for debate as virtually all carbonatites contain evidence for having crystallised from an alkali-bearing melt [Yaxley et al. 2022]. The claim that alkali-free liquids were propelled into the air and crystallised into calcite is questionable on the basis that alkali-free carbonatite melts probably do not even occur in nature, at least in the geological environments in which these rocks are found—associated with alkaline silicate rocks.

A commonly invoked argument for the existence of mobile calcite carbonatite lavas is the lack of any alkali carbonates in the extrusive rocks [Keller 1989; Bailey 1990]. Our experiments demonstrate that the sodic components of natrocarbonatites can be completely replaced and disappear within months (Figure 8). Therefore, any attempt to find such alkali carbonates in surface rocks from deep geological time is futile, and lack of thereof should not be taken as evidence for the primary nature of volcanic calcite carbonatites. We argue that this is the case for even relatively recent carbonatite eruptions, such as those in Cape Verde, Polino, or Fort Portal [Eby et al. 2009; Mourão et al. 2010; Rosatelli et al. 2010] where nyerereite is absent, but calcite contains minor elements indicative of a secondary origin as described above (i.e. P, Ba, Na, K; Table 4). Another main argument against an altered natrocarbonatite origin for extrusive calcite carbonatites was that alteration of nyerereite is accompanied by volume changes, either loss by dissolution or gain by transformation to pirssonite, that is expected to erase volcanic textures [Mitchell and Dawson 2021]. This includes delicate textures such as droplet-shaped lapilli stones. However, our dissolution experiments showed no increase in volume, and complete preservation of magmatic textures, including menisci and gas bubbles (Figures 2, 8). We also note that nyerereite in calcite-saturated rocks is likely to contain more $CaCO_3$ compared to gregoryite-saturated rocks, yielding more calcite upon alkali dissolution (Figure 4A). Given that dissolution can preserve volcanic textures, previously-existing and newly-formed cavities can be easily cemented with additional calcite [e.g. Barker 2007; Campeny et al. 2014], leading to complete fossilisation of primary natrocarbonatites in the form of calcite carbonatites. As the phenocryst phase in our experiments was calcite, not nyerereite, we could not directly test the nyerereite phenocryst pseudomorph hypothesis. Nonetheless, we observed three textural varieties of calcite in most experiments: (1) subhedral tabular calcite phenocrysts, (2) elongated calcite quench crystals, and (3) fine-grained euhedral calcite replacing groundmass nyerereite. These textures are typical for many purported calcite carbonatite lavas, but we conclude that these lavas were probably calcite-saturated natrocarbonatites. These carbonatite melt compositions are expected to be common because experimentally-determined liquid lines of descent lead to them [Figure 4B; Weidendorfer et al. 2017]. We suggest that most extrusive carbonatites found in the geological record were initially similar, and only acquired their almost pure calcitic composition after alteration [see further support for post-magmatic modification in the oxygen isotope study of Fosu et al. 2021]. It follows that Oldoinyo Lengai is likely to be an exceptionally rich sodic anomaly [Guzmics et al. 2019] saturated with nyerereite and gregoryite, and not representative of most extrusive carbonatites which are likely to

be at nyerereite and calcite saturation, with gregoryite merely being an uncommon accessory mineral.

6 Conclusions

Most of the controversy in the carbonatite literature concerned two endmember models for extrusive calcite carbonatites; (1) calcitic lavas with calcite phenocrysts can exist on the surface [Gittins and Jago 1991; Bailey 1993], or conversely that (2) calcite is replacement of nyerereite, whether as phenocryst or in the groundmass [Dawson et al. 1987]. The middle-ground view that calcite can replace nyerereite of multiple textural forms as well as coexist in the same rock as primary phenocrystic crystals has been frequently suggested or implied [Zaitsev et al. 2013], but was often excluded from the mainstream debate between the "calcitizers" and their opposing interlocutors. This oversight is clearly demonstrated by Mitchell and Dawson [2021] who wrote that "*… melts … crystallised calcite as a primary liquidus phase, and thus cannot differentiate to natrocarbonatite*", erroneously implying that calcite and natrocarbonatites are mutually exclusive. On the other hand, Campeny et al. [2015] report tabular calcite with concentric zoning observed in cathodoluminescence, which in our view is phenocrystic calcite, yet they interpret it as calcitic replacement of nyerereite [Campeny et al. 2015].

Our results demonstrate that natrocarbonatite liquids with calcite phenocrysts can undoubtedly exist. Here, we show that the middle-ground is feasible, and we suggest that most extrusive carbonatites—presently dominated by calcite—record a process in which calcite- and nyerereite-bearing natrocarbonatites erupted and their liquid fractions crystallised into mostly nyerereite (sequestering most chemical components of the lava) and accessory phases (mostly halides and sulfates sequestering elements excluded from nyerererite). Nyerereite is subsequently replaced by calcite with minimal volume changes such that magmatic textures are preserved, creating illusive "calcitic lavas". We affirm the suspicion of Bailey [1993] that calcite-saturated natrocarbonatites exist. Moreover, we believe that they are the rule rather than the exception. Since the term "natrocarbonatite" is often understood to refer to the calcite-free Oldoinyo Lengai lavas (although the recent formal definition of Yaxley et al. [2022] imposes no such calcite-free condition), and the term "calcite carbonatite" is often understood to refer to plutonic rocks, we suggest that the unaltered varieties of these extrusive rocks be termed "calcite natrocarbonatites", and their current alkali-free forms could be referred to as "altered calcite natrocarbonatites".

We suggest the following criteria for identification of various altered calcite natrocarbonatite constituents:

1. Semi-rounded or tabular calcite with SrO and no other minor elements (except perhaps REE charge-balanced by a monovalent cation) indicate equilibrium phenocrysts present at high temperature.

2. Elongated calcite, either isolated or growing from tabular calcite, indicate calcite crystallising upon rapid cooling or quench from a $CaCO_3$ component dissolved in the natrocarbonatite liquid during eruption. These quench calcites are likely to be compositionally similar to calcite phenocrysts.

3. Fine-grained calcite, potentially rhombohedral or trigonal, with minor BaO, Na_2O, K_2O, or P_2O_5, indicates direct replacement of nyerereite. Strontium is often present as well, but not diagnostic. Individual calcite grains might be zoned, with Ba variation the largest contributor to variable BSE brightness. We suggest that if this calcite appears to pseudomorph a mineral, then it replaces nyerereite phenocrysts. If it forms part of the groundmass, then it replaces nyerereite groundmass. Both forms can coexist in the same rock.

4. Clear calcite, pure or with minor Mg and Mn, that occurs interstitially, in veins, or as cavity fillings is likely to form late calcite with externally-introduced $CaCO_3$, and did not participate in the alteration process.

We note that these criteria are based on crystal morphology and composition. A thorough study of any carbonatite locality will benefit from additional methods such as trace element analysis, cathodoluminescence, and stable isotopes [Stoppa et al. 2023].

Author Contributions

INA conducted the high temperature experiments and their chemical analysis. MA conducted the low temperature experiments and their chemical analysis. MA wrote the paper with substantial input from INA. We thank Sam Broom-Fendley and an anonymous reviewer for valuable suggestions which improved the manuscript.

Acknowledgements

MA acknowledges the support of Australian Research Council project LP190100635. INA conducted the experiments during a visit to the Australian National University supported by a Future Research Talent (Indonesia) Award. We thank Michael Förster for his assistance with Raman spectroscopy. The authors acknowledge the instruments and expertise of Microscopy Australia (ROR: 042mm0k03) at the Centre for Advanced Microscopy, Australian National University, a facility enabled by NCRIS and university support.

Data Availability

All data is available in the paper.

Copyright Notice

References

Andersen, T. (2008). "Coexisting silicate and carbonatitic magmas in the Qassiarsuk Complex, Gardar Rift, Southwest Greenland". *The Canadian Mineralogist* 46(4), pages 933–950. DOI: 10.3749/canmin.46.4.933.

Andreeva, I. A. (2014). "Carbonatitic melts in olivine and magnetite from rare-metal carbonatite of the Belaya Zima alkaline carbonatite complex (East Sayan, Russia)". *Doklady Earth Sciences* 455(2), pages 436–440. DOI: 10.1134/s1028334x14050018.

Andreeva, I. A., V. I. Kovalenko, and N. N. Kononkova (2006). "Natrocarbonatitic melts of the Bol'shaya Tagna Massif, the Eastern Sayan region". *Doklady Earth Sciences* 408(1), pages 542–546. DOI: 10.1134/s1028334x06040088.

Anenburg, M. and T. Guzmics (2023). "Silica is unlikely to be soluble in upper crustal carbonatite melts". *Nature Communications* 14(1), page 942. DOI: 10.1038/s41467-023-35840-6.

Anenburg, M., J. A. Mavrogenes, C. Frigo, and F. Wall (2020). "Rare earth element mobility in and around carbonatites controlled by sodium, potassium, and silica". *Science Advances* 6(41), eabb6570. DOI: 10.1126/sciadv.abb6570.

Anenburg, M. and J. B. Walters (2024). "Metasomatic ijolite, glimmerite, silicocarbonatite, and antiskarn formation: carbonatite and silicate phase equilibria in the system Na_2O–CaO–K_2O–FeO–MgO–Al_2O_3–SiO_2–H_2O–O_2–CO_2". *Contributions to Mineralogy and Petrology* 179(5), page 40. DOI: 10.1007/s00410-024-02109-0.

Bailey, D. K. (1990). "Mantle carbonatite eruptions: Crustal context and implications". *Lithos* 26(1–2), pages 37–42. DOI: 10.1016/0024-4937(90)90039-4.

– (1993). "Carbonate magmas". *Journal of the Geological Society* 150(4), pages 637–651. DOI: 10.1144/gsjgs.150.4.0637.

Bambi, A. C. J. M., A. Costanzo, A. O. Gonçalves, and J. C. Melgarejo (2012). "Tracing the chemical evolution of primary pyrochlore from plutonic to volcanic carbonatites: the role of fluorine". *Mineralogical Magazine* 76(2), pages 377–392. DOI: 10.1180/minmag.2012.076.2.07.

Barker, D. S. (1989). "Field relations of carbonatites". *Carbonatites: genesis and evolution*. Edited by K. Bell. London: Unwin-Hyman, pages 39–69.

Barker, D. S. (2007). "Origin of cementing calcite in "carbonatite" tuffs". *Geology* 35(4), pages 371–374. DOI: 10.1130/g22957a.1.

Barker, D. S. and P. H. Nixon (1989). "High-Ca, low-alkali carbonatite volcanism at Fort Portal, Uganda". *Contributions to Mineralogy and Petrology* 103(2), pages 166–177. DOI: 10.1007/bf00378502.

Baudouin, C. and L. France (2023). "Trace-element partitioning between gregoryite, nyerereite, and natrocarbonatite melt: implications for natrocarbonatite evolution". *Contributions to Mineralogy and Petrology* 178(7), page 40. DOI: 10.1007/s00410-023-02021-z.

Berkesi, M., E. Bali, R. J. Bodnar, Á. Szabó, and T. Guzmics (2020). "Carbonatite and highly peralkaline nephelinite melts from Oldoinyo Lengai Volcano, Tanzania: The role of natrite-normative fluid degassing". *Gondwana Research* 85, pages 76–83. DOI: 10.1016/j.gr.2020.03.013.

Berkesi, M., J. L. Myovela, G. M. Yaxley, and T. Guzmics (2023). "Carbonatite formation in continental settings via high pressure–high temperature liquid immiscibility". *Geochimica et Cosmochimica Acta* 349, pages 41–54. DOI: 10.1016/j.gca.2023.03.027.

Campeny, M., V. S. Kamenetsky, J. C. Melgarejo, J. Mangas, J. Manuel, P. Alfonso, M. B. Kamenetsky, A. C. J. M. Bambi, and A. O. Gonçalves (2015). "Carbonatitic lavas in Catanda (Kwanza Sul, Angola): Mineralogical and geochemical constraints on the parental melt". *Lithos* 232, pages 1–11. DOI: 10.1016/j.lithos.2015.06.016.

Campeny, M., J. Mangas, J. C. Melgarejo, A. Bambi, P. Alfonso, T. Gernon, and J. Manuel (2014). "The Catanda extrusive carbonatites (Kwanza Sul, Angola): an example of explosive carbonatitic volcanism". *Bulletin of Volcanology* 76(4), page 818. DOI: 10.1007/s00445-014-0818-6.

Capaccioni, B. and F. Cuccoli (2005). "Spatter and welded air fall deposits generated by fire-fountaining eruptions: Cooling of pyroclasts during transport and deposition". *Journal of Volcanology and Geothermal Research* 145(3–4), pages 263–280. DOI: 10.1016/j.jvolgeores.2005.02.001.

Chayka, I. F., V. S. Kamenetsky, N. V. Vladykin, A. Kontonikas-Charos, I. R. Prokopyev, S. Y. Stepanov, and S. P. Krasheninnikov (2021). "Origin of alkali-rich volcanic and alkali-poor intrusive carbonatites from a common parental magma". *Scientific Reports* 11(1), page 17627. DOI: 10.1038/s41598-021-97014-y.

Chen, W., V. S. Kamenetsky, and A. Simonetti (2013). "Evidence for the alkaline nature of parental carbonatite melts at Oka complex in Canada". *Nature Communications* 4(1), page 2687. DOI: 10.1038/ncomms3687.

Christy, A. G., I. V. Pekov, and S. V. Krivovichev (2021). "The distinctive mineralogy of carbonatites". *Elements* 17(5), pages 333–338. DOI: 10.2138/gselements.17.5.333.

Clarke, M. G. C. and B. Roberts (1986). "Carbonated melilitites and calcitized alkalicarbonatites from Homa Mountain, western Kenya: a reinterpretation". *Geological Magazine* 123(6), pages 683–692. DOI: 10.1017/s0016756800024195.

Cooper, A. F., J. Gittins, and O. F. Tuttle (1975). "The system Na_2CO_3–K_2CO_3–$CaCO_3$ at 1 kilobar and its significance in carbonatite petrogenesis". *American Journal of Science* 275(5), pages 534–560. DOI: 10.2475/ajs.275.5.534.

Dawson, J. B. (1962). "Sodium carbonate lavas from Oldoinyo Lengai, Tanganyika". *Nature* 195(4846), pages 1075–1076. DOI: 10.1038/1951075a0.

– (1964a). "Carbonate tuff cones in Northern Tanganyika". *Geological Magazine* 101(2), pages 129–137. DOI: 10.1017/s0016756800048561.

– (1964b). "Carbonatitic volcanic ashes in Northern Tanganyika". *Bulletin Volcanologique* 27(1), pages 81–91. DOI: 10.1007/bf02597513.

– (1989). "Sodium carbonatite extrusions from Oldoinyo Lengai, Tanzania: Implications for carbonatite complex genesis". *Carbonatites: genesis and evolution*. Edited by K. Bell. London: Unwin-Hyman, pages 255–277.

– (1993). "A supposed sövite from Oldoinyo Lengai, Tanzania: result of extreme alteration of alkali carbonatite lava". *Mineralogical Magazine* 57(386), pages 93–101. DOI: 10.1180/minmag.1993.057.386.09.

Dawson, J. B., M. S. Garson, and B. Roberts (1987). "Altered former alkalic carbonatite lava from Oldoinyo Lengai, Tanzania: Inferences for calcite carbonatite lavas". *Geology* 15(8), pages 765–767. DOI: 10.1130/0091-7613(1987)15<765:AFACLF>2.0.CO;2.

Dawson, J. B., H. Pinkerton, G. E. Norton, and D. M. Pyle (1990). "Physicochemical properties of alkali carbonatite lavas: Data from the 1988 eruption of Oldoinyo Lengai, Tanzania". *Geology* 18(3), pages 260–263. DOI: 10.1130/0091-7613(1990)018<0260:PPOACL>2.3.CO;2.

Deans, T. and B. Roberts (1984). "Carbonatite tuffs and lava clasts of the Tinderet foothills, western Kenya: a study of calcified natrocarbonatites". *Journal of the Geological Society* 141(3), pages 563–580. DOI: 10.1144/gsjgs.141.3.0563.

Du Bois, C. G. B., J. Furst, N. J. Guest, and D. J. Jennings (1963). "Fresh natro carbonatite lava from Oldoinyo L'engai". *Nature* 197(4866), pages 445–446. DOI: 10.1038/197445a0.

Eby, G. N., F. E. Lloyd, and A. R. Woolley (2009). "Geochemistry and petrogenesis of the Fort Portal, Uganda, extrusive carbonatite". *Lithos* 113(3–4), pages 785–800. DOI: 10.1016/j.lithos.2009.07.010.

Fosu, B. R., P. Ghosh, T. B. Weisenberger, S. Spürgin, and S. G. Viladkar (2021). "A triple oxygen isotope perspective on the origin, evolution, and diagenetic alteration of carbonatites". *Geochimica et Cosmochimica Acta* 299, pages 52–68. DOI: 10.1016/j.gca.2021.01.037.

Frankis, E. J. and D. McKie (1973). "Subsolidus relations in the system Na_2CO_3–$CaCO_3$–H_2O". *Nature Physical Science* 246(155), pages 124–126. DOI: 10.1038/physci246124a0.

Galan, I., F. P. Glasser, and C. Andrade (2012). "Calcium carbonate decomposition". *Journal of Thermal Analysis and Calorimetry* 111(2), pages 1197–1202. DOI: 10.1007/s10973-012-2290-x.

Gittins, J. and R. E. Harmer (1997). "Dawson's Oldoinyo Lengai calciocarbonatite: a magmatic sövite or an extremely altered natrocarbonatite?" *Mineralogical Magazine* 61(406), pages 351–355. DOI: 10.1180/minmag.1997.061.406.02.

Gittins, J. and B. C. Jago (1991). "Extrusive carbonatites: their origins reappraised in the light of new experimental data". *Geological Magazine* 128(4), pages 301–305. DOI: 10.1017/s001675680001757x.

Gittins, J. and R. H. Mitchell (2023). "The genesis of calcite and dolomite carbonatite-forming magma by liquid immiscibility: a critical appraisal". *Geological Magazine* 160(8), pages 1463–1480. DOI: 10.1017/s001675682300050x.

Golovin, A. V., A. V. Korsakov, P. N. Gavryushkin, A. N. Zaitsev, V. G. Thomas, and B. N. Moine (2017a). "Raman spectra of nyerereite, gregoryite, and synthetic pure $Na_2Ca(CO_3)_2$: diversity and application for the study micro inclusions". *Journal of Raman Spectroscopy* 48(11), pages 1559–1565. DOI: 10.1002/jrs.5143.

Golovin, A. V., A. V. Korsakov, and A. N. Zaitsev (2015). "In situ ambient and high-temperature Raman spectroscopic studies of nyerereite $(Na, K)_2Ca(CO_3)_2$: can hexagonal zemkorite be stable at earth-surface conditions?" *Journal of Raman Spectroscopy* 46(10), pages 904–912. DOI: 10.1002/jrs.4756.

Golovin, A. V., I. S. Sharygin, and A. V. Korsakov (2017b). "Origin of alkaline carbonates in kimberlites of the Siberian craton: Evidence from melt inclusions in mantle olivine of the Udachnaya-East pipe". *Chemical Geology* 455, pages 357–375. DOI: 10.1016/j.chemgeo.2016.10.036.

Guzmics, T., M. Berkesi, R. J. Bodnar, A. Fall, E. Bali, R. Milke, E. Vetlényi, and C. Szabó (2019). "Natrocarbonatites: A hidden product of three-phase immiscibility". *Geology* 47(6), pages 527–530. DOI: 10.1130/g46125.1.

Guzmics, T., R. H. Mitchell, C. Szabó, M. Berkesi, R. Milke, and R. Abart (2011). "Carbonatite melt inclusions in coexisting magnetite, apatite and monticellite in Kerimasi calciocarbonatite, Tanzania: melt evolution and petrogenesis". *Contributions to Mineralogy and Petrology* 161(2), pages 177–196. DOI: 10.1007/s00410-010-0525-z.

Hay, R. L. (1978). "Melilitite–carbonatite tuffs in the Laetolil Beds of Tanzania". *Contributions to Mineralogy and Petrology* 67(4), pages 357–367. DOI: 10.1007/bf00383296.

– (1983). "Natrocarbonatite tephra of Kerimasi volcano, Tanzania". *Geology* 11(10), pages 599–602. DOI: 10.1130/0091-7613(1983)11<599:NTOKVT>2.0.CO;2.

– (1989). "Holocene carbonatite–nephelinite tephra deposits of Oldoinyo Lengai, Tanzania". *Journal of Volcanology and Geothermal Research* 37(1), pages 77–91. DOI: 10.1016/0377-0273(89)90114-5.

Hayward, C. L. and A. P. Jones (1991). "Cathodoluminescence petrography of middle Proterozoic extrusive carbonatite from Qasiarsuk, South Greenland". *Mineralogical Magazine* 55(381), pages 591–603. DOI: 10.1180/minmag.1991.055.381.12.

Hernanz, A., J. M. Gavira-Vallejo, J. F. Ruiz-López, and H. G. M. Edwards (2008). "A comprehensive micro-Raman spectroscopic study of prehistoric rock paintings from the Sierra de las Cuerdas, Cuenca, Spain". *Journal of Raman Spectroscopy* 39(8), pages 972–984. DOI: 10.1002/jrs.1940.

Hobley, C. W. (1918). "A volcanic eruption in East Africa". *The Journal of the East Africa and Uganda Natural History Society* 6(13), pages 339–343. URL: https://archive.org/details/journalof131519181919east/page/338.

Hubberten, H.-W., K. Katz-Lehnert, and J. Keller (1988). "Carbon and oxygen isotope investigations in carbonatites and related rocks from the Kaiserstuhl, Germany". *Chemical Geology* 70(3), pages 257–274. DOI: 10.1016/0009-2541(88)90097-6.

Innocenzi, F., S. Ronca, S. Foley, S. Agostini, and M. Lustrino (2024). "Carbonatite and ultrabasic magmatism at Toro Ankole and Virunga, western branch of the East African Rift system". *Gondwana Research* 125, pages 317–342. DOI: 10.1016/j.gr.2023.09.005.

Jacobson, N. S., B. Fegley, J. A. Setlock, and G. Costa (2020). "Solubility of water in carbonatites". *ACS Earth and Space Chemistry* 4(11), pages 2144–2152. DOI: 10.1021/acsearthspacechem.0c00222.

Káldos, R., T. Guzmics, R. H. Mitchell, J. B. Dawson, R. Milke, and C. Szabó (2015). "A melt evolution model for Kerimasi volcano, Tanzania: Evidence from carbonate melt inclusions in jacupirangite". *Lithos* 238, pages 101–119. DOI: 10.1016/j.lithos.2015.09.011.

Kamenetsky, V. S., A. G. Doroshkevich, H. A. L. Elliott, and A. N. Zaitsev (2021). "Carbonatites: Contrasting, complex, and controversial". *Elements* 17(5), pages 307–314. DOI: 10.2138/gselements.17.5.307.

Karunadasa, K. S. P., C. H. Manoratne, H. M. T. G. A. Pitawala, and R. M. G. Rajapakse (2019). "Thermal decomposition of calcium carbonate (calcite polymorph) as examined by in-situ high-temperature X-ray powder diffraction". *Journal of Physics and Chemistry of Solids* 134, pages 21–28. DOI: 10.1016/j.jpcs.2019.05.023.

Katz, K. and J. Keller (1981). "Comb-layering in carbonatite dykes". *Nature* 294(5839), pages 350–352. DOI: 10.1038/294350a0.

Keller, J. (1989). "Extrusive carbonatites and their significance". *Carbonatites: genesis and evolution*. Edited by K. Bell. London: Unwin-Hyman, pages 70–88.

Keller, J. and A. N. Zaitsev (2006). "Calciocarbonatite dykes at Oldoinyo Lengai, Tanzania: the fate of natrocarbonatite". *The Canadian Mineralogist* 44(4), pages 857–876. DOI: 10.2113/gscanmin.44.4.857.

Keller, J. (1981). "Carbonatitic volcanism in the Kaiserstuhl alkaline complex: Evidence for highly fluid carbonatitic melts at the Earth's surface". *Journal of Volcanology and Geothermal Research* 9(4), pages 423–431. DOI: 10.1016/0377-0273(81)90048-2.

Keller, J. and M. Krafft (1990). "Effusive natrocarbonatite activity of Oldoinyo Lengai, June 1988". *Bulletin of Volcanology* 52(8), pages 629–645. DOI: 10.1007/bf00301213.

Keppler, H. (2003). "Water solubility in carbonatite melts". *American Mineralogist* 88(11–12), pages 1822–1824. DOI: 10.2138/am-2003-11-1224.

Kjarsgaard, B. A., D. L. Hamilton, and T. D. Peterson (1995). "Peralkaline nephelinite/carbonatite liquid immiscibility: Comparison of phase compositions in experiments and natural lavas from Oldoinyo Lengai". *Carbonatite Volcanism*. Edited by K. Bell and J. Keller. Springer Berlin Heidelberg, pages 163–190. ISBN: 9783642791826. DOI: 10.1007/978-3-642-79182-6_13.

Kogarko, L. N., D. A. Plant, C. M. B. Henderson, and B. A. Kjarsgaard (1991). "Na-rich carbonate inclusions in perovskite and calzirtite from the Guli intrusive Ca-carbonatite, polar Siberia". *Contributions to Mineralogy and Petrology* 109(1), pages 124–129. DOI: 10.1007/bf00687205.

Le Bas, M. J. (1981). "Carbonatite magmas". *Mineralogical Magazine* 44(334), pages 133–140. DOI: 10.1180/minmag.1981.044.334.02.

– (1987). "Nephelinites and carbonatites". *Geological Society, London, Special Publications* 30(1), pages 53–83. DOI: 10.1144/gsl.sp.1987.030.01.05.

Le Bas, M. J. and J. A. Dixon (1965). "A new carbonatite in the Legetet Hills, Kenya". *Nature* 207(4992), pages 68–68. DOI: 10.1038/207068a0.

Lee, W.-J. and P. J. Wyllie (1997). "Liquid immiscibility in the join $NaAlSiO_4$–$NaAlSi_3O_8$–$CaCO_3$ at 1 GPa: Implications for crustal carbonatites". *Journal of Petrology* 38(9), pages 1113–1135. DOI: 10.1093/petroj/38.9.1113.

Lee, W.-J. and P. J. Wyllie (1996). "Liquid immiscibility in the join $NaAlSi_3O_8$–$CaCO_3$ to 2.5 GPa and the origin of calciocarbonatite magmas". *Journal of Petrology* 37(5), pages 1125–1152. DOI: 10.1093/petrology/37.5.1125.

Lundstrom, C. C., R. Hervig, T. P. Fischer, M. Sivaguru, L. Yin, Z. Zhou, X. Lin, and R. Grossi-Diniz (2022). "Insight into differentiation in alkalic systems: Nephelinite–carbonate–water experiments aimed at Ol Doinyo Lengai carbonatite genesis". *Frontiers in Earth Science* 10, page 970264. DOI: 10.3389/feart.2022.970264.

Macdonald, R., B. A. Kjarsgaard, I. P. Skilling, G. R. Davies, D. L. Hamilton, and S. Black (1993). "Liquid immiscibility between trachyte and carbonate in ash flow tuffs from Kenya". *Contributions to Mineralogy and Petrology* 114(2), pages 276–287. DOI: 10.1007/bf00307762.

Mariano, A. N. and P. L. Roeder (1983). "Kerimasi: A Neglected Carbonatite Volcano". *The Journal of Geology* 91(4), pages 449–455. URL: https://www.jstor.org/stable/30064003.

Mitchell, R. H. (2005). "Carbonatites and carbonatites and carbonatites". *The Canadian Mineralogist* 43(6), pages 2049–2068. DOI: 10.2113/gscanmin.43.6.2049.

Mitchell, R. H. and B. A. Kjarsgaard (2008). "Experimental studies of the system $Na_2Ca(CO_3)_2$–NaCl–KCl at 0.1 GPa: Implications for the differentiation and low-temperature crystallization of natrocarbonatite". *The Canadian Mineralogist* 46(4), pages 971–980. DOI: 10.3749/canmin.46.4.971.

Mitchell, R. H. and J. B. Dawson (2021). "Mineralogy of volcanic calciocarbonatites from the Trig Point Hill debris flow, Kerimasi volcano, Tanzania: implications for the altered natrocarbonatite hypothesis". *Mineralogical Magazine* 85(4), pages 484–495. DOI: 10.1180/mgm.2020.97.

Mourão, C., J. Mata, R. Doucelance, J. Madeira, A. B. d. Silveira, L. C. Silva, and M. Moreira (2010). "Quaternary extrusive calciocarbonatite volcanism on Brava Island (Cape Verde): A nephelinite–carbonatite immiscibility product". *Journal of African Earth Sciences* 56(2–3), pages 59–74. DOI: 10.1016/j.jafrearsci.2009.06.003.

Ngwenya, B. T. and D. K. Bailey (1990). "Kaluwe carbonatite, Zambia: an alternative to natrocarbonatite". *Journal of the Geological Society* 147(2), pages 213–216. DOI: 10.1144/gsjgs.147.2.0213.

Nielsen, T. F. D., I. P. Solovova, and I. V. Veksler (1997). "Parental melts of melilitolite and origin of alkaline carbonatite: evidence from crystallised melt inclusions, Gardiner complex". *Contributions to Mineralogy and Petrology* 126(4), pages 331–344. DOI: 10.1007/s004100050254.

O'Neill, H. S. C. and M. I. Pownceby (1993). "Thermodynamic data from redox reactions at high temperatures. II. The MnO–Mn_3O_4 oxygen buffer, and implications for the thermodynamic properties of MnO and Mn_3O_4". *Contributions to Mineralogy and Petrology* 114(3), pages 315–320. DOI: 10.1007/bf01046534.

Panina, L. I. (2005). "Multiphase carbonate-salt immiscibility in carbonatite melts: data on melt inclusions from the Krestovskiy massif minerals (Polar Siberia)". *Contributions to Mineralogy and Petrology* 150(1), pages 19–36. DOI: 10.1007/s00410-005-0001-3.

Pecora, W. T. (1956). "Carbonatites: A review". *Geological Society of America Bulletin* 67(11), page 1537. DOI: 10.1130/0016-7606(1956)67[1537:car]2.0.co;2.

Peterson, T. D. (1990). "Petrology and genesis of natrocarbonatite". *Contributions to Mineralogy and Petrology* 105(2), pages 143–155. DOI: 10.1007/bf00678981.

Pirajno, F. and H.-C. Yu (2022). "The carbonatite story once more and associated REE mineral systems". *Gondwana Research* 107, pages 281–295. DOI: 10.1016/j.gr.2022.03.006.

Prokopyev, I. R., A. G. Doroshkevich, D. V. Zhumadilova, A. E. Starikova, Y. N. Nugumanova, and N. V. Vladykin (2021). "Petrogenesis of Zr–Nb (REE) carbonatites from the Arbarastakh complex (Aldan Shield, Russia): Mineralogy and inclusion data". *Ore Geology Reviews* 131, page 104042. DOI: 10.1016/j.oregeorev.2021.104042.

Prokopyev, I., E. Kozlov, E. Fomina, A. Doroshkevich, and M. Dyomkin (2020). "Mineralogy and fluid regime of formation of the REE–late-stage hydrothermal mineralization of Petyayan-Vara carbonatites (Vuoriyarvi, Kola Region, NW Russia)". *Minerals* 10(5), page 405. DOI: 10.3390/min10050405.

Rapprich, V., B. F. Walter, V. Kopačková-Strnadová, T. Kluge, B. Čejková, O. Pour, J. M. Hora, J. Kynický, and T. Magna (2024). "Gravitational collapse of a volcano edifice as a trigger for explosive carbonatite eruption?" *Geological Society of America Bulletin* 136(5–6), pages 2291–2304. DOI: 10.1130/b37013.1.

Riley, T. R., D. K. Bailey, and F. E. Lloyd (1996). "Extrusive carbonatite from the Quaternary Rockeskyll complex, West Eifel, Germany". *Canadian Mineralogist* 34(2), pages 389–401. URL: https://pubs.geoscienceworld.org/mac/canmin/article/34/2/389/12757/.

Rosatelli, G., F. Wall, and M. J. Le Bas (2003). "Potassic glass and calcite carbonatite in lapilli from extrusive carbonatites at Rangwa Caldera Complex, Kenya". *Mineralogical Magazine* 67(5), pages 931–955. DOI: 10.1180/0026461036750152.

Rosatelli, G., F. Wall, F. Stoppa, and M. Brilli (2010). "Geochemical distinctions between igneous carbonate, calcite cements, and limestone xenoliths (Polino carbonatite, Italy): spatially resolved LAICPMS analyses". *Contributions to Mineralogy and Petrology* 160(5), pages 645–661. DOI: 10.1007/s00410-010-0499-x.

Stoppa, F. and A. Cundari (1995). "A new Italian carbonatite occurrence at Cupaello (Rieti) and its genetic significance". *Contributions to Mineralogy and Petrology* 122(3), pages 275–288. DOI: 10.1007/s004100050127.

Stoppa, F., S. Cirilli, A. Sorci, S. Broom-Fendley, C. Principe, M. G. Perna, and G. Rosatelli (2023). "Igneous and sedimentary 'limestones': the puzzling challenge of a converging classification". *Geological Society, London, Special Publications* 520(1), pages 327–352. DOI: 10.1144/sp520-2021-120.

Toscani, L., E. Salvioli-Mariani, M. Mattioli, C. Tellini, T. Boschetti, P. Iacumin, and E. Selmo (2020). "The pyroclastic breccia of the Cabezo Negro de Tallante (SE Spain): The first finding of carbonatite volcanism in the Internal Domain of the Betic Cordillera". *Lithos* 354–355, page 105288. DOI: 10.1016/j.lithos.2019.105288.

Turner, D. C. (1988). "Volcanic carbonatites of the Kaluwe complex, Zambia". *Journal of the Geological Society* 145(1), pages 95–106. DOI: 10.1144/gsjgs.145.1.0095.

Veksler, I. V., T. F. D. Nielsen, and S. V. Sokolov (1998). "Mineralogy of crystallized melt inclusions from Gardiner and Kovdor ultramafic alkaline complexes: Implications for carbonatite genesis". *Journal of Petrology* 39(11–12), pages 2015–2031. DOI: 10.1093/petroj/39.11-12.2015.

Von Knorring, O. and C. G. B. du Bois (1961). "Carbonatitic lava from Fort Portal area in western Uganda". *Nature* 192(4807), pages 1064–1065. DOI: 10.1038/1921064b0.

Walter, B. F., R. J. Giebel, M. Steele-MacInnis, M. A. Marks, J. Kolb, and G. Markl (2021). "Fluids associated with carbonatitic magmatism: A critical review and implications for carbonatite magma ascent". *Earth-Science Reviews* 215, page 103509. DOI: 10.1016/j.earscirev.2021.103509.

Watkinson, D. H. and P. J. Wyllie (1971). "Experimental study of the composition join $NaAlSiO_4$–$CaCO_3$–H_2O and the Genesis of alkalic rock–carbonatite complexes". *Journal of Petrology* 12(2), pages 357–378. DOI: 10.1093/petrology/12.2.357.

Weidendorfer, D., M. W. Schmidt, and H. B. Mattsson (2017). "A common origin of carbonatite magmas". *Geology* 45(6), pages 507–510. DOI: 10.1130/g38801.1.

Woolley, A. R., M. W. C. Barr, V. K. Din, G. C. Jones, F. Wall, and C. T. Williams (1991). "Extrusive carbonatites from the Uyaynah area, United Arab Emirates". *Journal of Petrology* 32(6), pages 1143–1167. DOI: 10.1093/petrology/32.6.1143.

Woolley, A. R. (2021). "Remembrance of carbonatites past". *Elements* 17(5), pages 367–368. DOI: 10.2138/gselements.17.5.367.

Wyllie, P. J. and E. J. Raynor (1965). "DTA and quenching methods in the system CaO–CO_2–H_2O". *American Mineralogist* 50(11–12), pages 2077–2082.

Wyllie, P. J. and O. F. Tuttle (1960). "The system CaO–CO_2–H_2O and the origin of carbonatites". *Journal of Petrology* 1(1), pages 1–46. DOI: 10.1093/petrology/1.1.1.

– (1962). "Carbonatitic lavas". *Nature* 194(4835), pages 1269–1269. DOI: 10.1038/1941269a0.

Yaxley, G. M., M. Anenburg, S. Tappe, S. Decree, and T. Guzmics (2022). "Carbonatites: Classification, sources, evolution, and emplacement". *Annual Review of Earth and Planetary Sciences* 50(1), pages 261–293. DOI: 10.1146/annurev-earth-032320-104243.

Zaitsev, A. and J. Keller (2006). "Mineralogical and chemical transformation of Oldoinyo Lengai natrocarbonatites, Tanzania". *Lithos* 91(1–4), pages 191–207. DOI: 10.1016/j.lithos.2006.03.018.

Zaitsev, A. N. (2010). "Nyerereite from calcite carbonatite at the Kerimasi Volcano, Northern Tanzania". *Geology of Ore Deposits* 52(7), pages 630–640. DOI: 10.1134/s1075701510070159.

Zaitsev, A. N., J. Keller, J. Spratt, T. E. Jeffries, and V. V. Sharygin (2009). "Chemical composition of nyerereite and gregoryite from natrocarbonatites of Oldoinyo Lengai volcano, Tanzania". *Geology of Ore Deposits* 51(7), pages 608–616. DOI: 10.1134/s1075701509070095.

Zaitsev, A. N., J. Keller, J. Spratt, E. N. Perova, and A. Kearsley (2008). "Nyerereite–pirssonite–calcite–shortite relationships in altered natrocarbonatites, Oldoinyo Lengai, Tanzania". *The Canadian Mineralogist* 46(4), pages 843–860. DOI: 10.3749/canmin.46.4.843.

Zaitsev, A. N., T. Wenzel, T. Vennemann, and G. Markl (2013). "Tinderet volcano, Kenya: an altered natrocarbonatite locality?" *Mineralogical Magazine* 77(3), pages 213–226. DOI: 10.1180/minmag.2013.077.3.01.

Zaitsev, V. A., L. N. Kogarko, and I. D. Ryabchikov (2003). "Carbonate globules in Cape Verde volcanics—evidence of preceding carbonate–silicate immiscibility". 4th EUROCARB Workshop. Canary Islands, Spain.